

AD-A059 712

ARMY ARMAMENT RESEARCH AND DEVELOPMENT COMMAND ABERD--ETC F/G 17/9
140-GHZ CAPTURE ANTENNA MULTIPATH EXPERIMENT.(U)
AUG 78 H B WALLACE

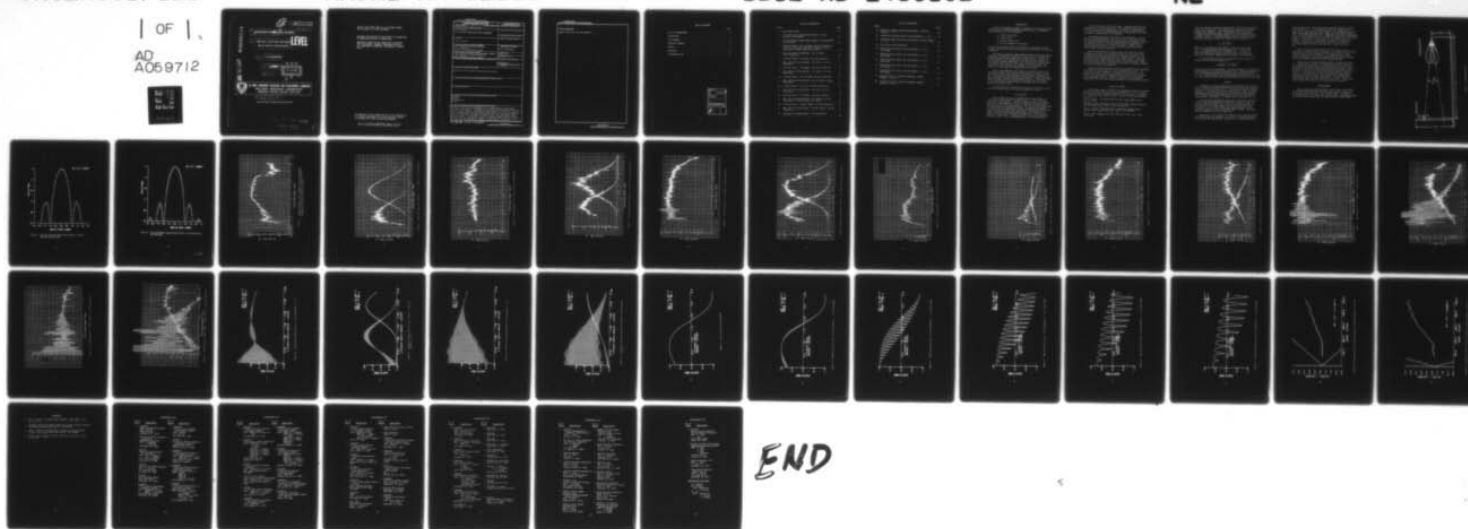
UNCLASSIFIED

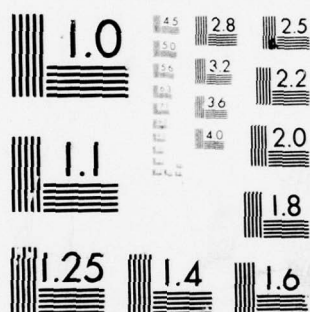
ARBRL-MR-02855

SBIE-AD-E430102

NL

| OF |
AD
A059712





MICROCOPY RESOLUTION TEST CHART
NATIONAL BUREAU OF STANDARDS-1963-A

AD A059712

DDC FILE COPY

12

19 AD-E430102

9 MEMORANDUM REPORT ARBRL-MR-02855

14

18 SBIE

6 140-GHz CAPTURE ANTENNA
MULTIPATH EXPERIMENT.

LEVEL II

10 H. Bruce Wallace

11 Aug 1978

DDC
RECEIVED
OCT 12 1978
B

12 48p.



US ARMY ARMAMENT RESEARCH AND DEVELOPMENT COMMAND
BALLISTIC RESEARCH LABORATORY
ABERDEEN PROVING GROUND, MARYLAND

16 1L162618AH80

Approved for public release; distribution unlimited.

78 09 01 030
392 471

mt

Destroy this report when it is no longer needed.
Do not return it to the originator.

Secondary distribution of this report by originating
or sponsoring activity is prohibited.

Additional copies of this report may be obtained
from the National Technical Information Service,
U.S. Department of Commerce, Springfield, Virginia
22161.

The findings in this report are not to be construed as
an official Department of the Army position, unless
so designated by other authorized documents.

*The use of trade names or manufacturers' names in this report
does not constitute indorsement of any commercial product.*

UNCLASSIFIED

SECURITY CLASSIFICATION OF THIS PAGE (When Data Entered)

REPORT DOCUMENTATION PAGE		READ INSTRUCTIONS BEFORE COMPLETING FORM
1. REPORT NUMBER MEMORANDUM REPORT ARBRL-MR-02855	2. GOVT ACCESSION NO.	3. RECIPIENT'S CATALOG NUMBER
4. TITLE (and Subtitle) 140-GHz CAPTURE ANTENNA MULTIPATH EXPERIMENT		5. TYPE OF REPORT & PERIOD COVERED
		6. PERFORMING ORG. REPORT NUMBER
7. AUTHOR(s) H. Bruce Wallace		8. CONTRACT OR GRANT NUMBER(s)
9. PERFORMING ORGANIZATION NAME AND ADDRESS US Army Ballistic Research Laboratory (ATTN: DRDAR-BLB) Aberdeen Proving Ground, MD 21005		10. PROGRAM ELEMENT, PROJECT, TASK AREA & WORK UNIT NUMBERS RDT&E 1L162618AH80
11. CONTROLLING OFFICE NAME AND ADDRESS US Army Armament Research and Development Command US Army Ballistic Research Laboratory (ATTN: DRDAR-BL) Aberdeen Proving Ground, MD 21005		12. REPORT DATE AUGUST 1978
		13. NUMBER OF PAGES 46
14. MONITORING AGENCY NAME & ADDRESS (if different from Controlling Office)		15. SECURITY CLASS. (of this report) UNCLASSIFIED
		15a. DECLASSIFICATION/DOWNGRADING SCHEDULE
16. DISTRIBUTION STATEMENT (of this Report) Approved for public release; distribution unlimited.		
17. DISTRIBUTION STATEMENT (of the abstract entered in Block 20, if different from Report)		
18. SUPPLEMENTARY NOTES		
19. KEY WORDS (Continue on reverse side if necessary and identify by block number) Multipath Beamrider Millimeter Wave Capture		
20. ABSTRACT (Continue on reverse side if necessary and identify by block number) As part of a study of the feasibility of a 140-GHz beamrider, measurements were made of the effect of multipath on the antenna power patterns of simulated missile capture antennas. The upper and lower lobes of two conically scanning capture antennas were simulated using 50.8-mm and 152.4-mm horn-lens antennas. Vertical field probes were made at a range of 100 m over high weeds, mowed grass and asphalt. A theoretical model for specular ground reflection compared favorably with the experimental results. On the basis of this model, it is concluded that the capture of a beamrider missile would be difficult at ranges		

DD FORM 1 JAN 73 1473 EDITION OF 1 NOV 65 IS OBSOLETE

UNCLASSIFIED

SECURITY CLASSIFICATION OF THIS PAGE (When Data Entered)

UNCLASSIFIED

SECURITY CLASSIFICATION OF THIS PAGE(When Data Entered)

Item 20 continued

greater than 200 m over some terrain.

UNCLASSIFIED

SECURITY CLASSIFICATION OF THIS PAGE(When Data Entered)

TABLE OF CONTENTS

	Page
LIST OF ILLUSTRATIONS.	5
INTRODUCTION	7
TEST SCENARIO.	7
THEORETICAL MODELS	8
RESULTS.	9
REFERENCES	40
DISTRIBUTION LIST.	41

ACCESSION for		
NTIS	White Section	<input checked="" type="checkbox"/>
DDC	Buff Section	<input type="checkbox"/>
UNANNOUNCED		<input type="checkbox"/>
JUSTIFICATION		
BY		
DISTRIBUTION/AVAILABILITY CODES		
Dist.	AVAIL	end/or SPECIAL
A		

LIST OF ILLUSTRATIONS

Figure	Page
1. Experimental Setup	11
2. 152.4-mm Diameter Antenna Power Pattern, E-Plane Measured and Simulated	12
3. 50.8-mm Diameter Antenna Power Pattern, E-Plane Measured and Simulated.	13
4. Tracking Pattern - CW, 1-m Weeds, 152.4-mm Transmitter (Above 3.3-m Receiver could not be aimed accurately, attenuation at lower levels due to weeds.)	14
5. Upper and Lower Lobe Patterns - CW, 1-m Weeds, 152.4-Transmitter.	15
6. Tracking Pattern - CW, Grass, 152.4-mm Transmitter	16
7. Upper and Lower Lobe Patterns - CW, Grass, 152.4-mm Transmitter.	17
8. Tracking Pattern - CW, Asphalt, 153.4-mm Transmitter	18
9. Upper and Lower Lobe Patterns - CW, Asphalt, 153.4-mm Transmitter.	19
10. Tracking Pattern - CW, 1-m weeds, 50.8-mm Transmitter.	20
11. Upper and Lower Lobe Patterns - CW, 1-m Weeds, 50.8-mm Transmitter.	21
12. Tracking Pattern - CW, Grass, 50.8-mm Transmitter.	22
13. Upper and Lower Lobe Patterns - CW, Grass, 50.8-mm Transmitter.	23
14. Tracking Pattern - CW, Asphalt, 50.8-mm Transmitter.	24
15. Upper and Lower Lobe Patterns - CW, Asphalt, 50.8-mm Transmitter. (LO lost from 3.5 to 3.85 m.).	25
16. Tracking Pattern - Pulsed, Asphalt, 50.8-mm Transmitter.	26
17. Upper and Lower Lobe Patterns - Pulsed, Asphalt, 50.8-mm Transmitter.	27
18. Theoretical Tracking Pattern - 152.4-mm Antenna, $\rho = -0.5$	28

LIST OF ILLUSTRATIONS

Figure		Page
19.	Theoretical Upper and Lower Lobe Patterns - 152.4-mm Antenna, $\rho = -0.5$	29
20.	Theoretical Tracking Pattern, 50.8-mm Antenna, $\rho = -0.5$. . .	30
21.	Theoretical Upper and Lower Lobe Patterns, 50.8-mm Antenna, $\rho = -0.5$	31
22.	Error Curve with No Multipath.	32
23.	Theoretical Error Curve, 152.4-mm Antenna, $\rho = -0.5$, 100-m Range.	33
24.	Theoretical Error Curve, 152.4-mm Antenna, $\rho = -0.5$, 200-m Range.	34
25.	Theoretical Error Curve, 152.4-mm Antenna, $\rho = -0.5$, 300-m Range.	35
26.	Theoretical Error Curve, 152.4-mm Antenna, $\rho = -0.5$, 400-m Range.	36
27.	Theoretical Error Curve, 152.4-mm Antenna, $\rho = -0.5$, 500-m Range.	37
28.	Theoretical Path of "Perfect" Beamrider, Antenna Diameter = 152.4 mm.	38
29.	Theoretical Path of "Perfect" Beamrider, Antenna Diameter = 50.8 mm	39

INTRODUCTION

The BRL has conducted a number of studies in-house concerning the feasibility of a 140-GHz beamrider antitank system. The beamrider system performs four basic functions:

- target acquisition,
- target track,
- missile capture, and
- missile guidance to the target.

In the "capture" mode, while the main beam is continually tracking a target, a beamriding missile is launched into the beam of a "capture" transmitter.

The capture transmitter beam contains encoded positioning information which is detected by a receiver in the tail of the missile and decoded to provide error signals for missile control. The missile is not tracked at any time but tries to seek the 3-db crossover of the conically scanned transmitter. The capture beam is aimed toward the tracking beam, which is also coded, so that the missile will intercept it and switch over to tracking its 3-db crossover. The missile will then ride the tracking beam to the target.

Part of the tradeoffs in the design of a capture system is the size of the "basket" the missile can be initially injected into and the effects of multipath reflection on the conically scanning beam null. By going to a small antenna, the basket can be made very large but the energy reflected from the ground increases. The ground reflection will change the power patterns of the upper and lower lobes of the capture beam causing either an elevation shift in the null position or multiple nulls.

This experiment was designed to get a general idea of the magnitude of multipath effects for various antennas and terrains.

TEST SCENARIO

A 100-m range was set up to measure the multipath effects on a conically scanning beam at 140-GHz (Figure 1). Three different earth covers were measured: high weeds, mowed weeds, and an asphalt road flat to approximately ± 1.3 cm. A conically scanning antenna smaller than 0.91 m was not available at the time for these experiments so single horn-lens antennas were used. The antenna was mounted on a precision altazimuth mount to permit positioning the transmitted beam to simulate the upper and lower lobes. The transmitter was placed 1.82 m above the ground and the beams had a 3-db crossover parallel to the ground. A 10-mW CW IMPATT oscillator was initially used as a source. Later measurements used a 0.5 W pulsed IMPATT.

At the other end of the 100-m range, a superheterodyne receiver was placed on a vertical positioner. The positioner could move the receiver from just above ground level to a height of approximately 4 m. The receiver was maintained parallel to the ground at all times and aimed in azimuth with a 7x riflescope.

Two different antennas were used for the transmitter - a 50.8-mm and a 150.4-mm horn-lens. The receiver used a 50.8-mm horn-lens. All of the measurements were made using vertical polarization. Prior to running the test, the one-way beam patterns were measured with the receiver elevated to 12 m above the ground. Figures 2 and 3 show the measured patterns (x's) and computer generated patterns (solid lines) of the two antennas.

Prior to measuring the simulated upper and lower lobes of the transmitter, the receiver was moved from the top of the positioner to ground level while the transmitter continually tracked it. This provided a baseline measurement of power and multipath. Since the positioner used a manually cranked winch, some noise was introduced into the receiver output from oscillation of the positioner. Aiming was difficult above the 3-m position and resulted in improper pointing in some of the pattern measurements.

After the tracking pattern was made, the transmitter was positioned to simulate the upper lobe and a power measurement was taken. The lower lobe was then simulated. A calibrated RF attenuator in the receiver was used to measure received power relative to the received power at the time when the transmitter was pointed at the receiver in its uppermost position. Figures 4 through 17 are the patterns measured for the 50.8- and 150.4-mm antennas over the different terrains.

THEORETICAL MODELS

The equations used to calculate the multipath will not be discussed here as they can be found in many other references.^{1,2,3,4} It should be pointed out that the ground reflections were assumed to be specular, i.e., the ground was perfectly smooth. Actually the ground roughness

¹David K. Barton, "Low-Angle Radar Tracking," Proc. IEEE, Vol 62, No. 6, Jun 74.

²Richard A. McGee, "Multipath Suppression by Swept Frequency Methods," BRL Memorandum Report 1950, Nov 68. (AD #682728)

³Cecil L. Wilson, "Pointing Errors in Sequential Lobing Antenna Systems," BRL Technical Note 1463, May 62. (AD #609009)

⁴Miles V. Klein, Optics, New York, John Wiley & Sons, Inc., 1970, pp 184-189.

serves to diminish the effects of multipath by diffusing the reflected energy over a broad area. The higher the RF frequency, the rougher a given terrain appears. Also any vegetation cover will tend to attenuate the reflected signal. These facts can be readily seen by comparing the 50.8-mm antenna patterns over high weeds and asphalt (Figures 10 and 15). Generally specular reflection applies if the RMS height variation in the first Fresnel zone of reflection is

$$\sigma_n < \frac{1}{8} \frac{\lambda}{\sin \theta},$$

where σ_n is the RMS height variation, θ is the reflection angle, and λ is the wavelength of the propagated beam.¹ In this case $\theta_{\max} = 3.3$ degrees (receivers + 4m height), $\lambda = 2.14$ mm, so if $\sigma_n^{\max} \leq 4.61$ mm specular reflection can be assumed. This case will be met for the asphalt surface but not for the two earth surfaces.

The antenna power patterns were simulated using a $[J_1(x)/(x)]^2$ function for the 50.8 mm antennas and a

$$\frac{2}{3} \left(\frac{\sin x}{x} \right)^2 + \frac{1}{3} \left(\frac{\sin x}{x} \right)^3$$

function for the 150.4-mm antenna. Very good agreement was obtained for both antennas as can be seen in Figures 2 and 3. Figures 18 through 21 show the expected multipath for the forward scattering coefficient $\rho = -0.5$. Relative power is the expected power received relative to the free space power received when the transmitter and receiver are coaligned.

RESULTS

A comparison of the measured data and theoretical model indicates that the forward scattering coefficients for the ground with vegetative cover is less than or equal to -0.1. This assumes a totally specular reflection. If a model was developed taking into account the surface roughness and diffuse reflection, ρ_0 would increase in the model but other reflection parameters would be introduced which would reduce the multipath. Over asphalt, ρ_0 appears to be on the order of -0.5.

An interesting phenomenon was noted when comparing the multipath in the CW and the chirped pulse measurements. Figure 15 shows 15 cycles of multipath between the 1- and 2-m vertical positions, for the CW source. The number agrees with the multipath model used. In Figure 17 only 13 cycles of multipath appear between 1 and 2 m when the pulsed source had a chirp from 139 to 140 GHz. The reason for this difference is not yet understood.

Based on $\rho_0 = -0.5$ a series of elevation error curves were generated to determine the capability of a missile to find the intended null point of the capture beam. Figure 22 is a representative error

curve generated for a 150.4-mm conically scanning antenna at a range of 100 m with $\rho_o = 0$. As the missile flies lower in the capture beam, the receiver would find the difference (Δ_p) between the contributions of the upper and lower lobes. Where Δ_p is zero should be the null. Since the transmitter is at a height of 1.82 m and is boresighted parallel to the ground, the null is at the same height without multipath present. If the missile is below the null, Δ_p is positive which would tell the missile to move upward. Conversely, if the missile is high, a negative Δ_p would tell the missile to move downward. All of the calculated error curves are for a receiver with an RF AGC.

Figure 23 shows the error curve at 100 m with $\rho_o = -0.5$. A second null is appearing due to multipath. At a range of 200 m (Figure 24) there are five nulls having positive slope, any one of which could be sought out by the missile. As we progress out in range (Figures 25 through 27) more nulls appear until the possible tracking nulls are outside the beam of the main tracking antenna.

Figures 28 and 29 show the computed path of a perfect missile, i.e., instantaneous response, when injected into capture beams from 152.4-mm and 50.8-mm antennas. In these simulations the free space boresight of the capture antenna was parallel to the ground. The missile was injected into the antenna beam before multipath affected the nulls. The missile will only follow nulls lying on a positive slope. It can be seen that for the 152.4-mm and 50.8-mm antennas the missile would fly outside the envelope of the tracking beam at approximately 300 m and 220 m, respectively. The 3-db envelopes of the capture beams are indicated by the solid lines. These ranges would increase for reduced ρ_o or increased antenna diameters.

ACKNOWLEDGMENT

The multipath experiment described in this report is the result of a number of persons in the Millimeter Wave Research Group at the Ballistic Research Laboratory. The equipment used was designed by Mr. Donald Bauerle, Mr. Joseph Knox, and the author. The computer model of multipath was developed with assistance from Mr. Richard McGee.

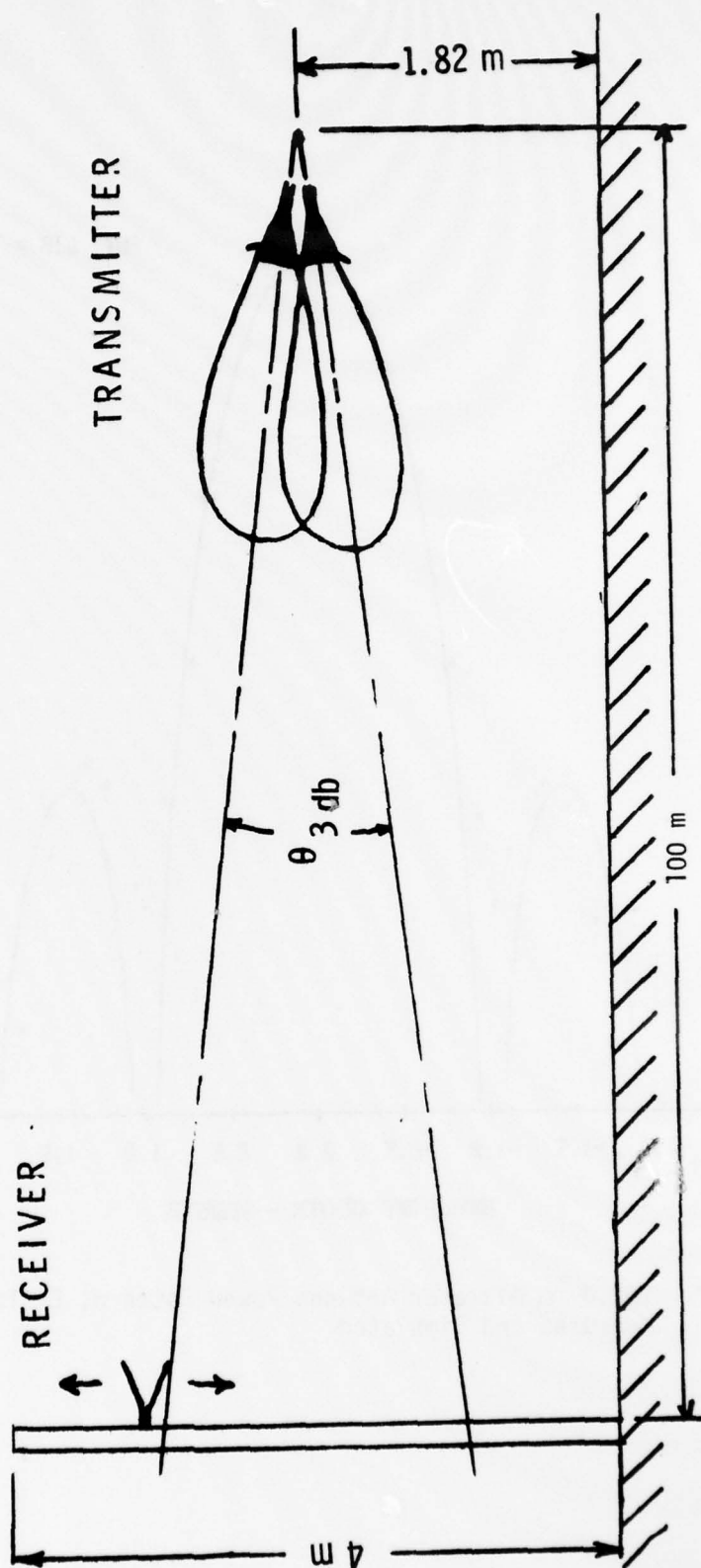


Figure 1. Experimental Setup

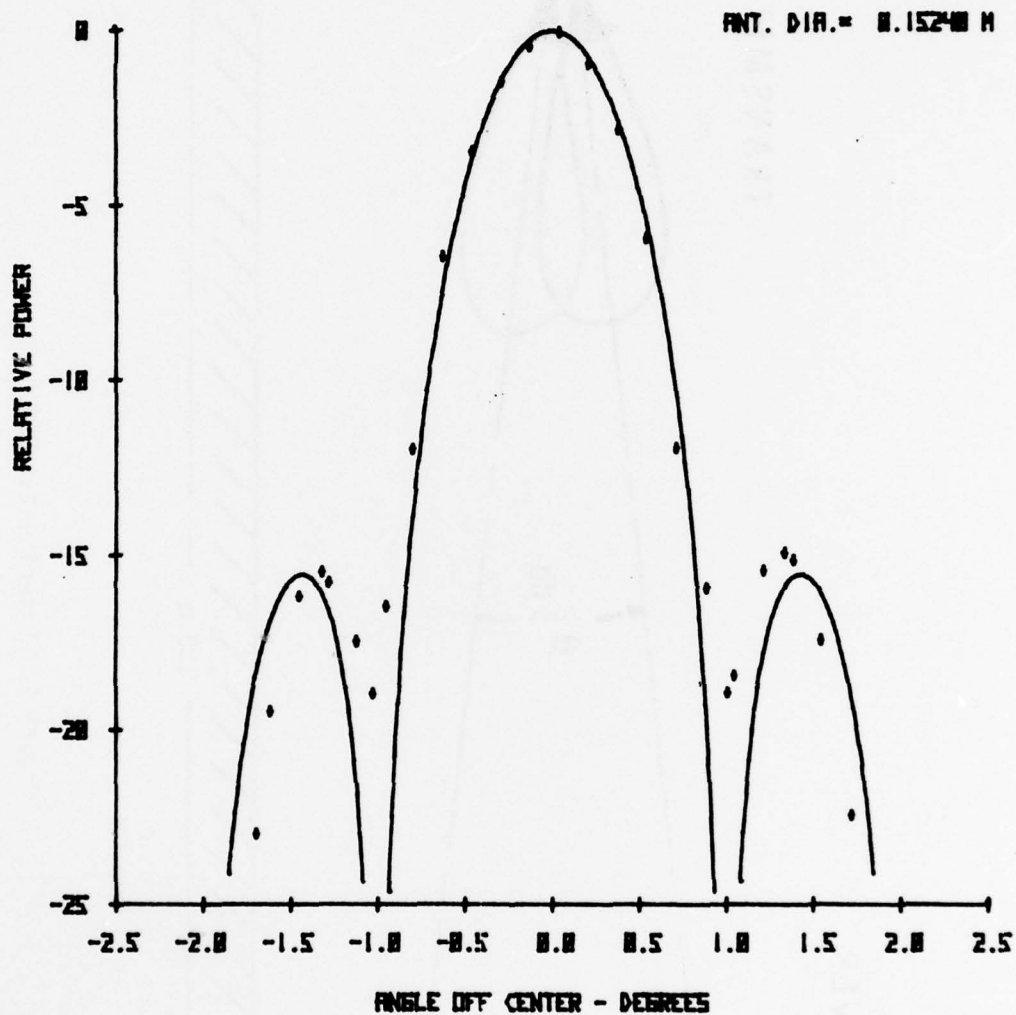


Figure 2. 152.4-mm Diameter Antenna Power Pattern, E-Plane
Measured and Simulated

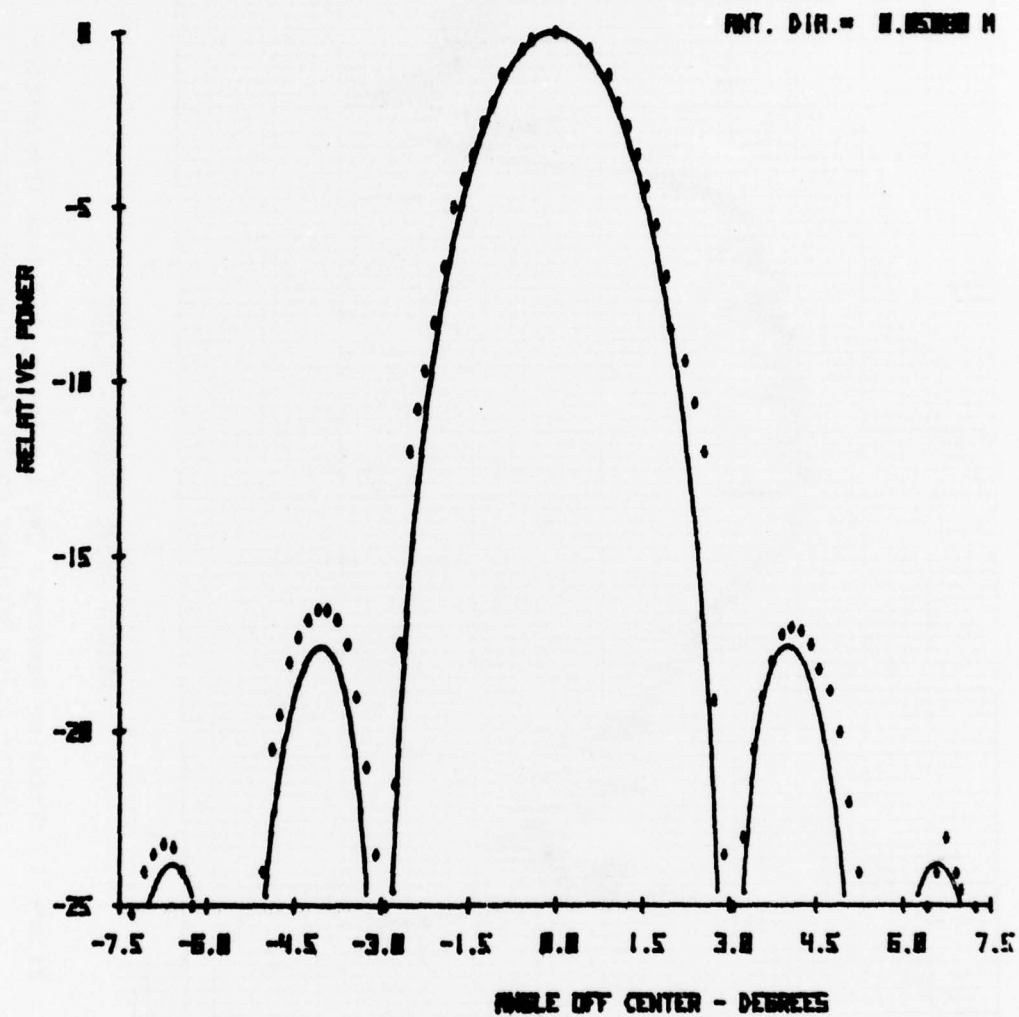


Figure 3. 50.8-mm Diameter Antenna Power Pattern, E-Plane Measured and Simulated

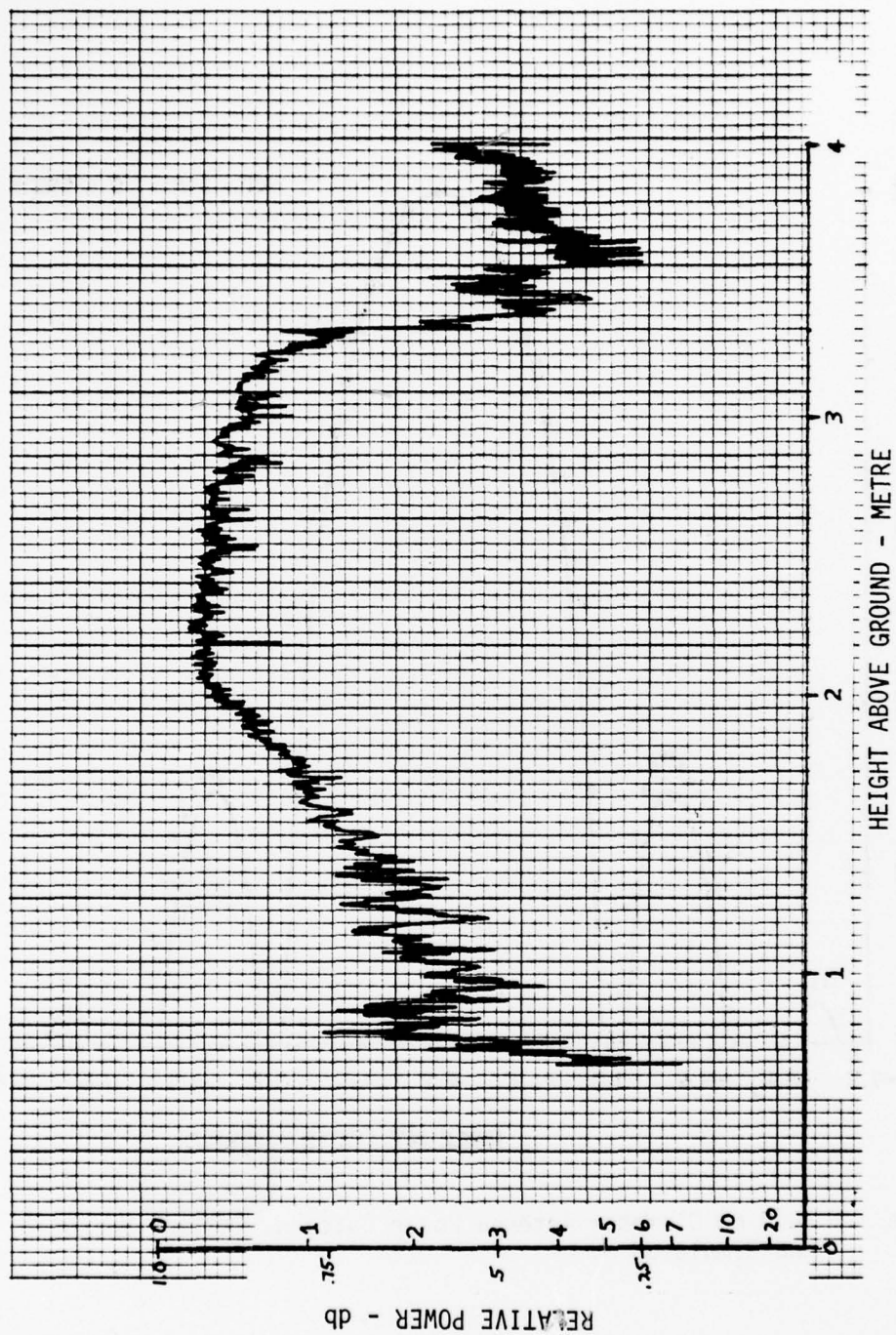


Figure 4. Tracking Pattern - CW, 1-m Weeds, 152.4-mm Transmitter
(Above 3.3-m Receiver could not be aimed accurately,
attenuation at lower levels due to weeds.)

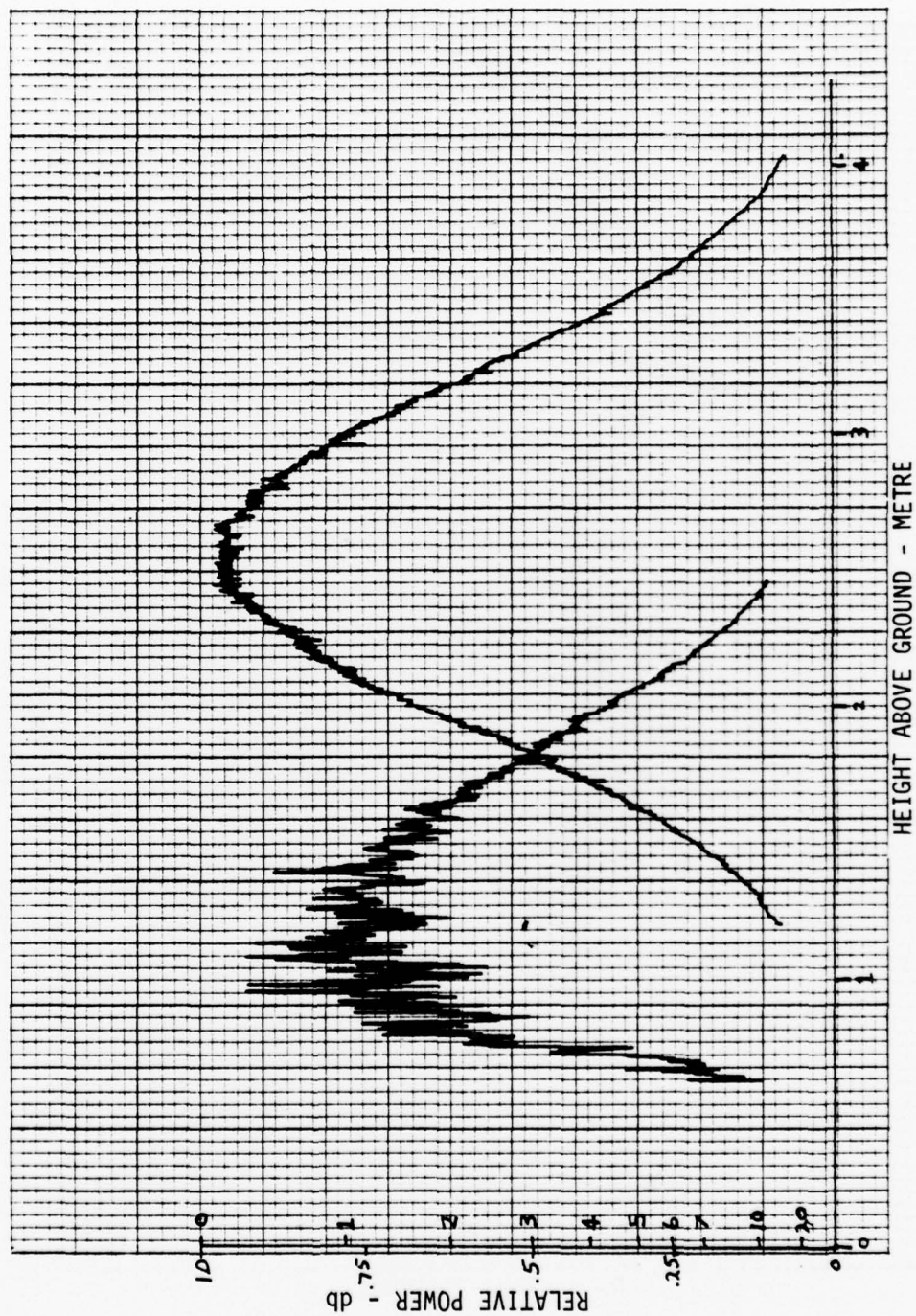


Figure 5. Upper and Lower Lobe Patterns - CW, 1-m Weeds, 152.4-Transmitter

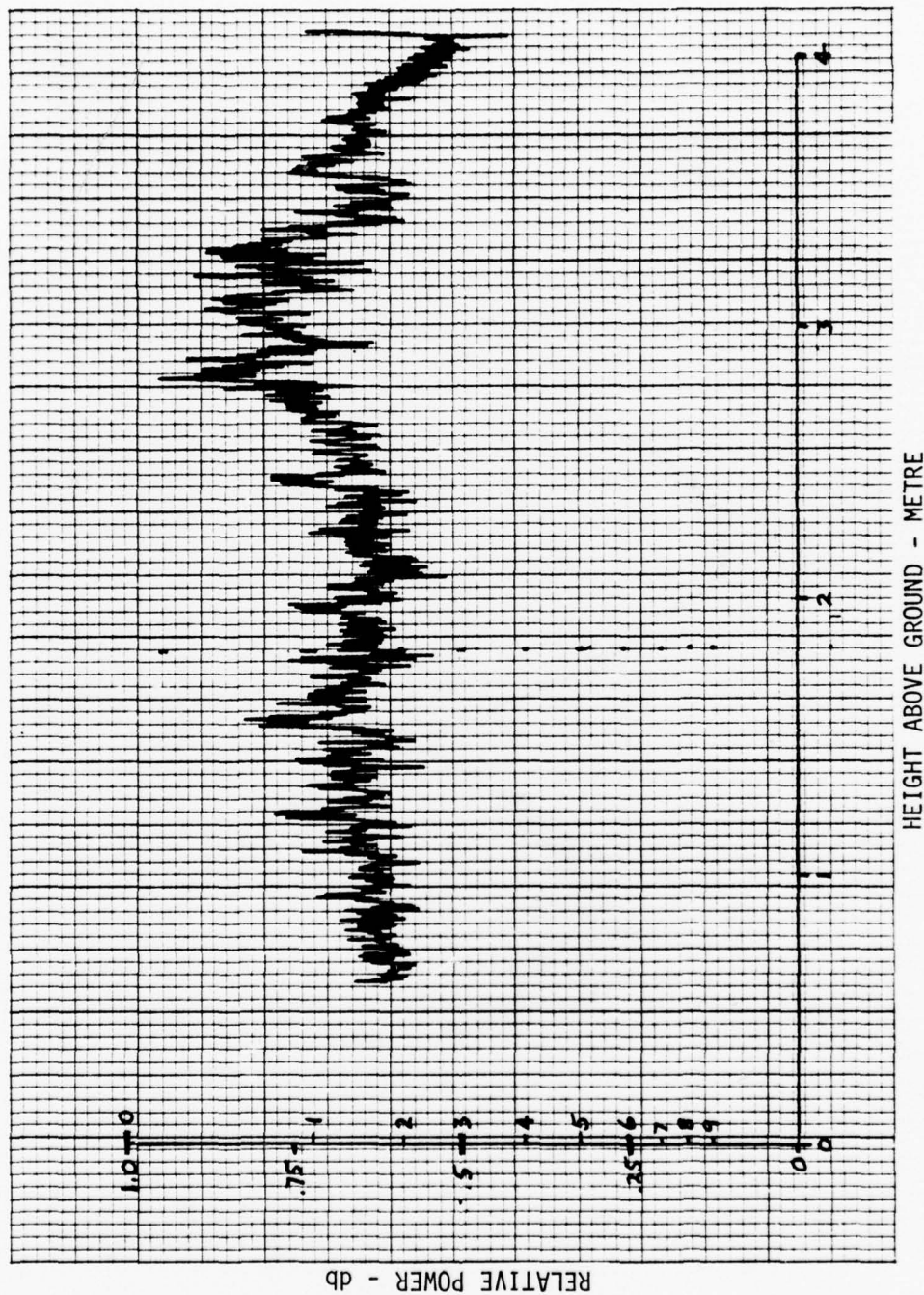


Figure 6. Tracking Pattern - CW, Grass, 152.4-mm Transmitter

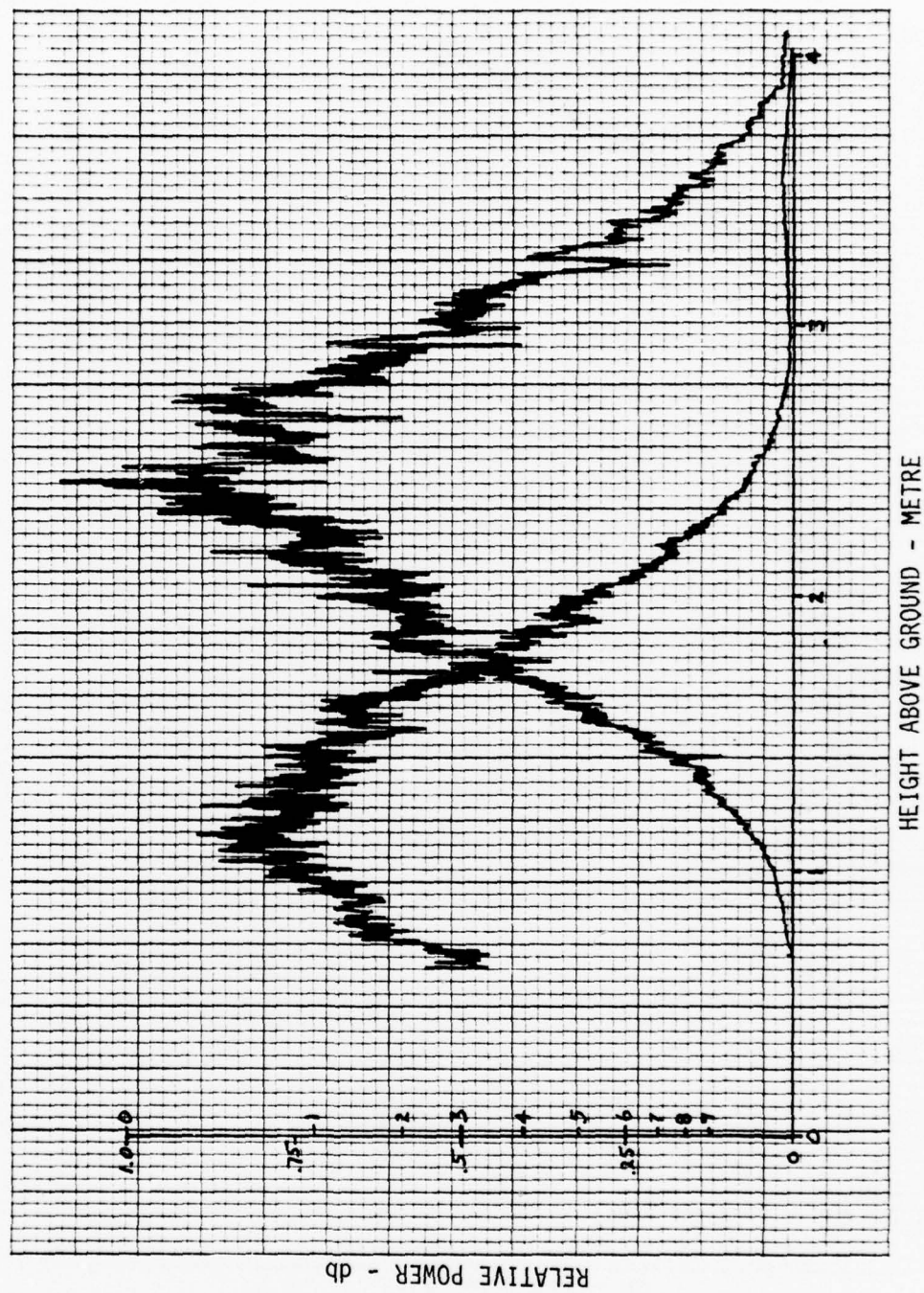


Figure 7. Upper and Lower Lobe Patterns - CW, Grass, 152.4-mm Transmitter

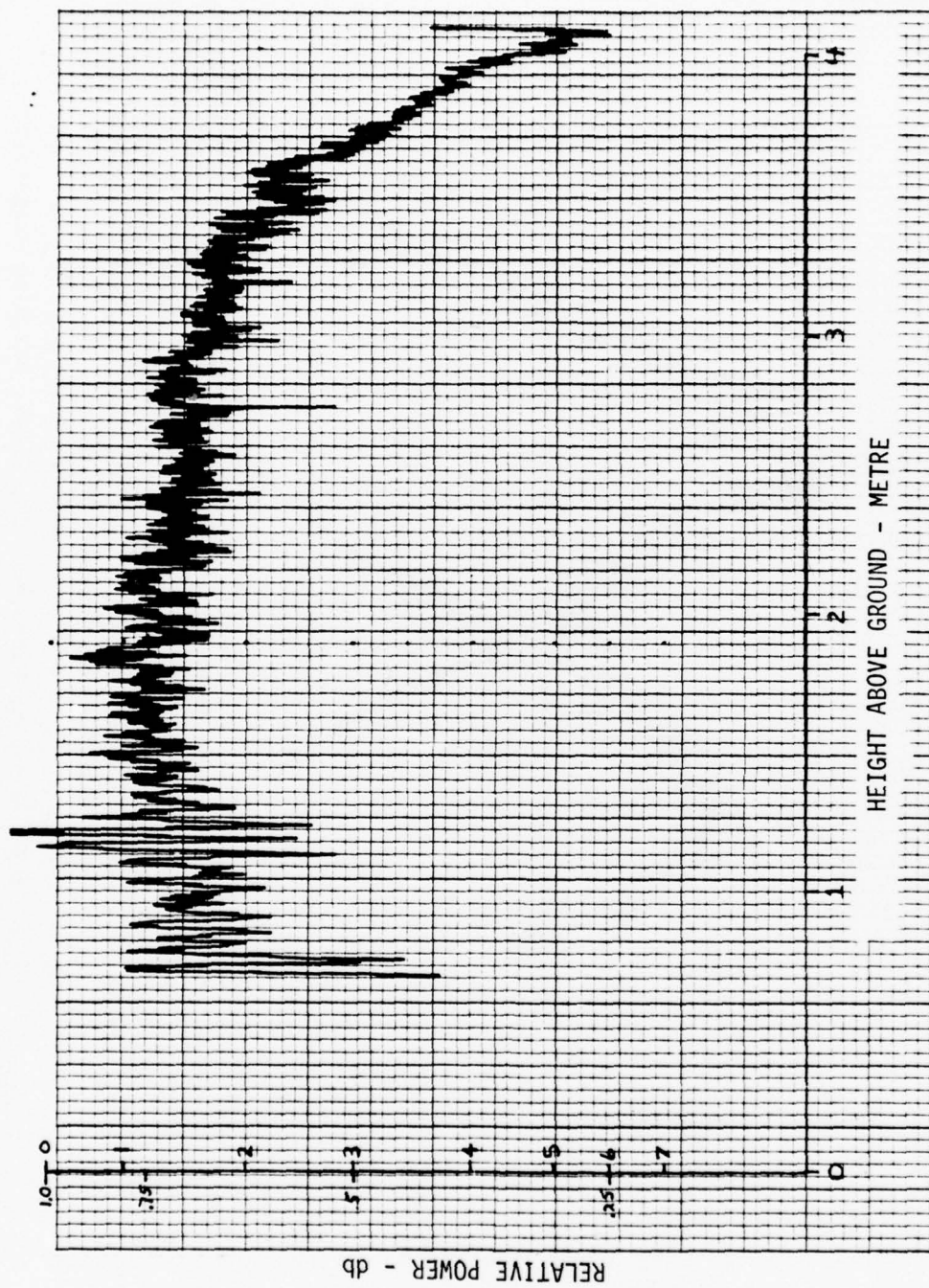


Figure 8. Tracking Pattern - CW, Asphalt, 153.4-mm Transmitter

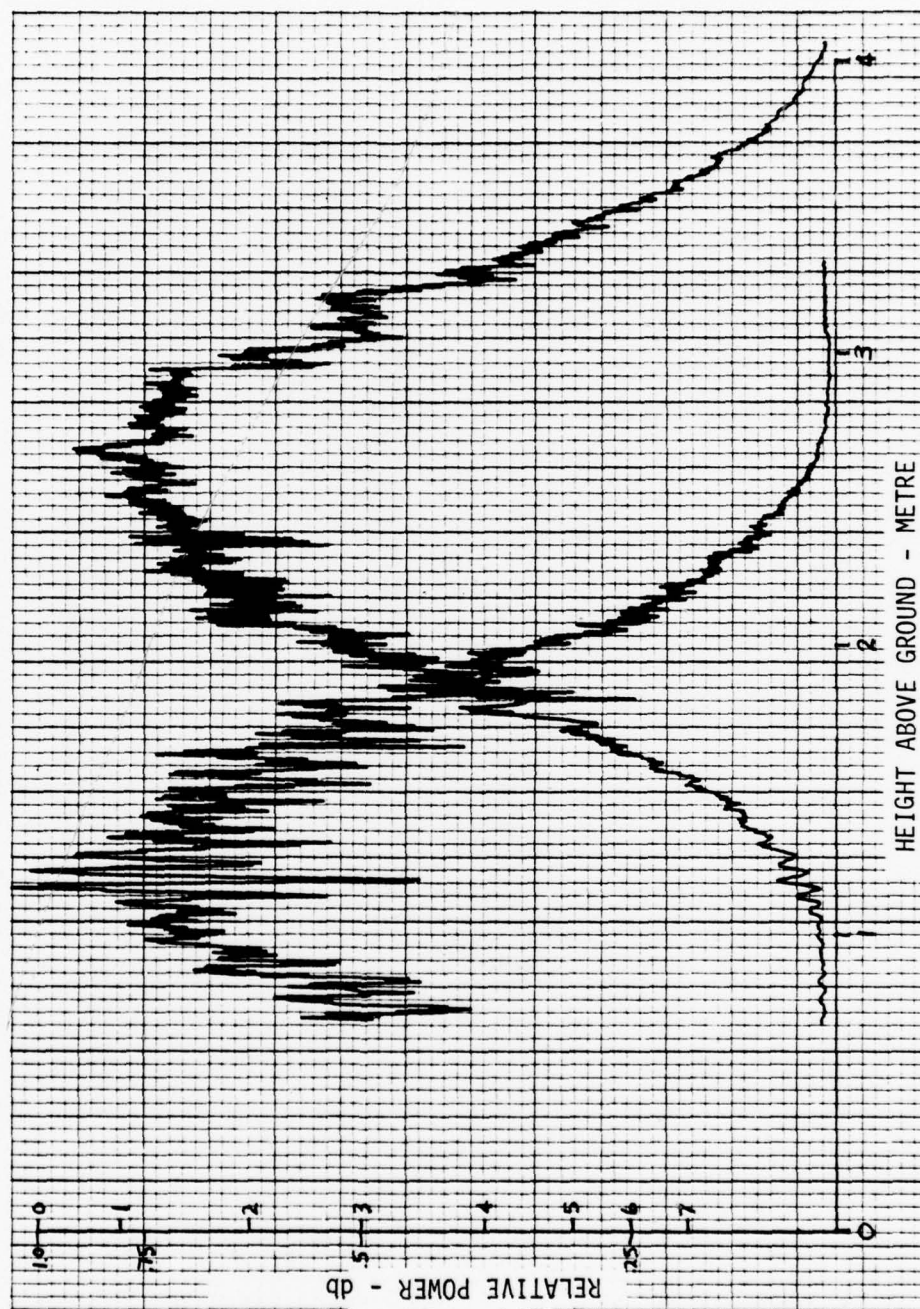


Figure 9. Upper and Lower Lobe Patterns - CW, Asphalt, 153.4-mm Transmitter

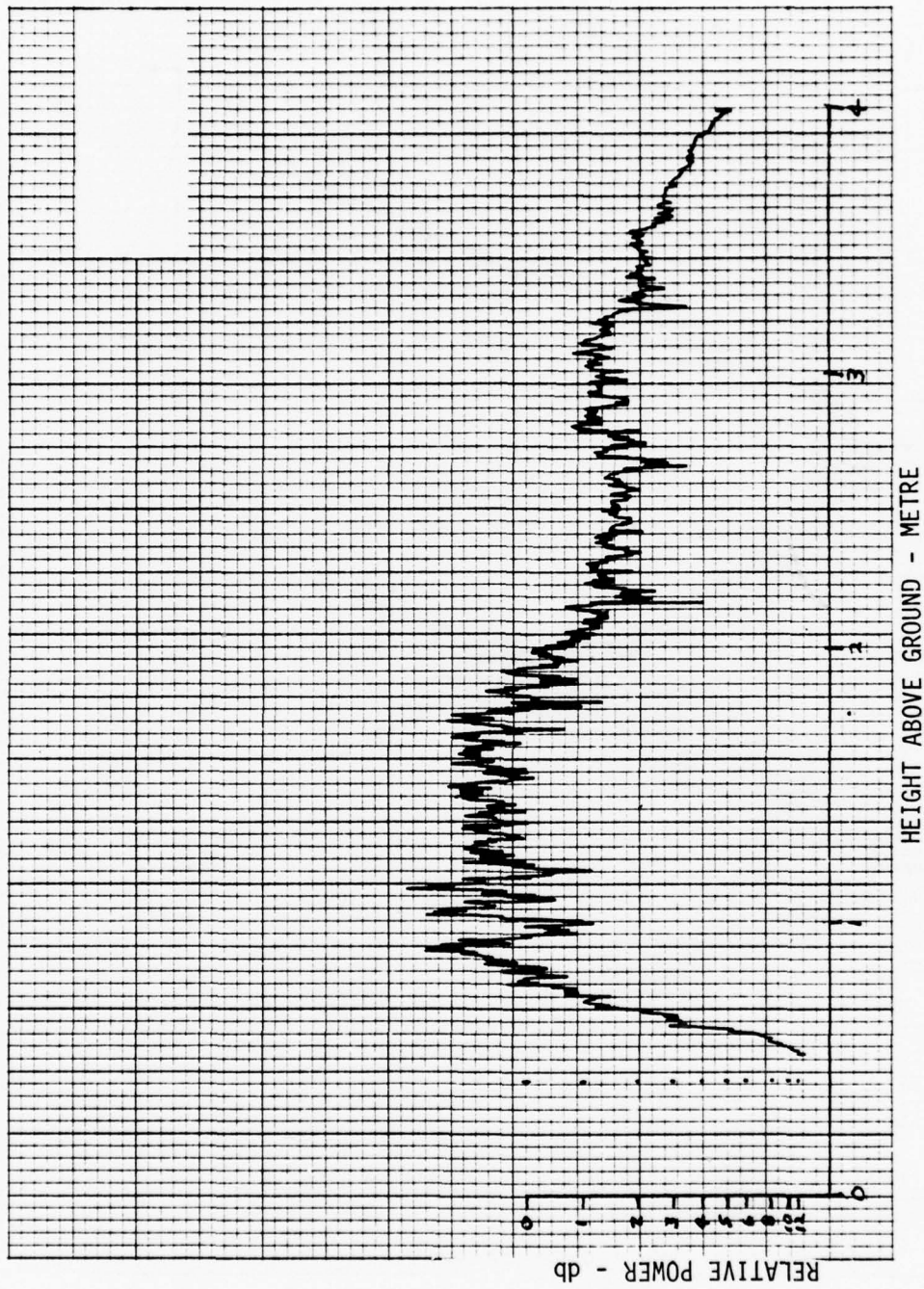


Figure 10. Tracking Pattern - CW, 1-m weeds, 50.8-mm Transmitter

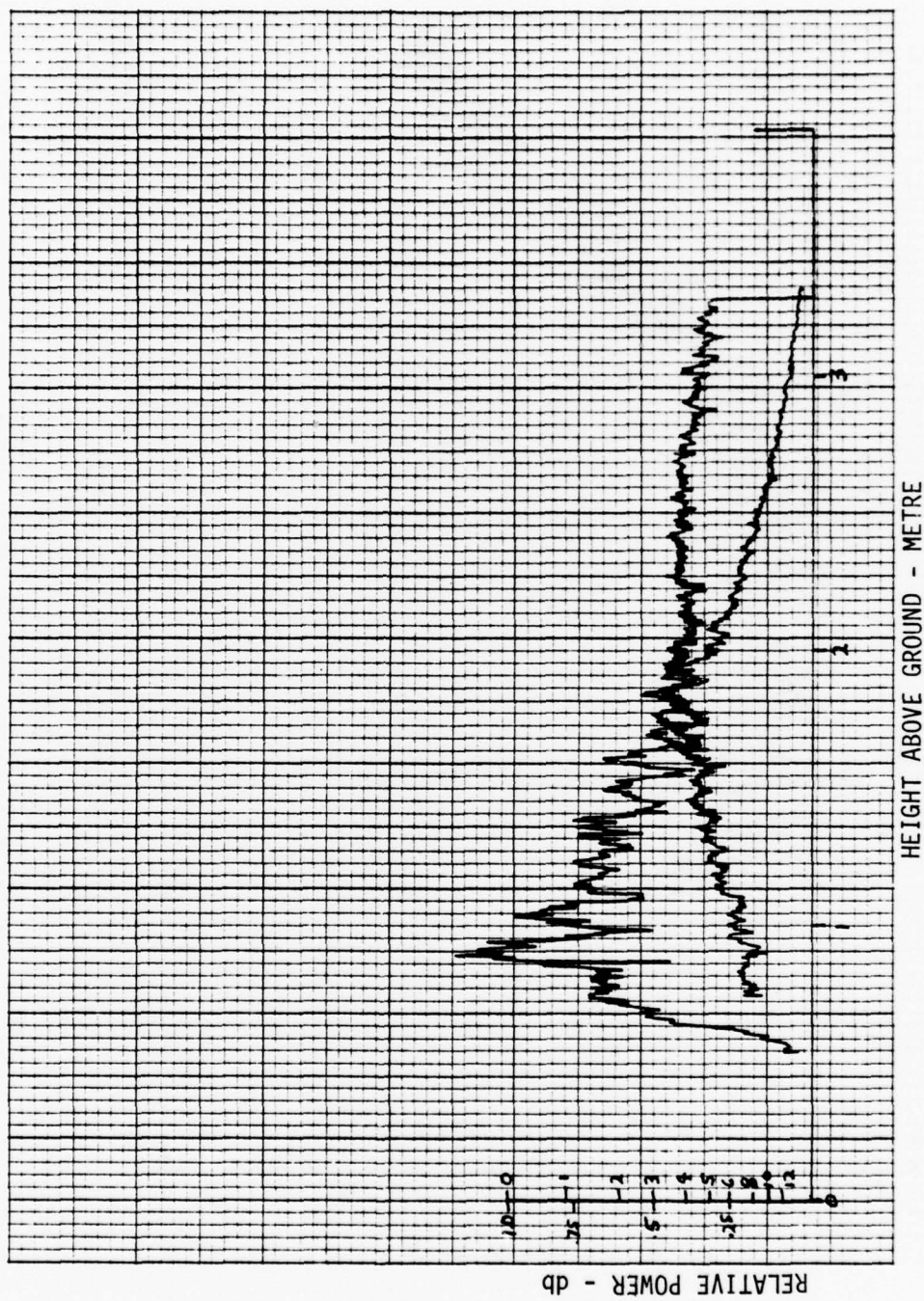


Figure 11. Upper and Lower Lobe Patterns - CW, 1-m Weeds, 50.8-mm Transmitter

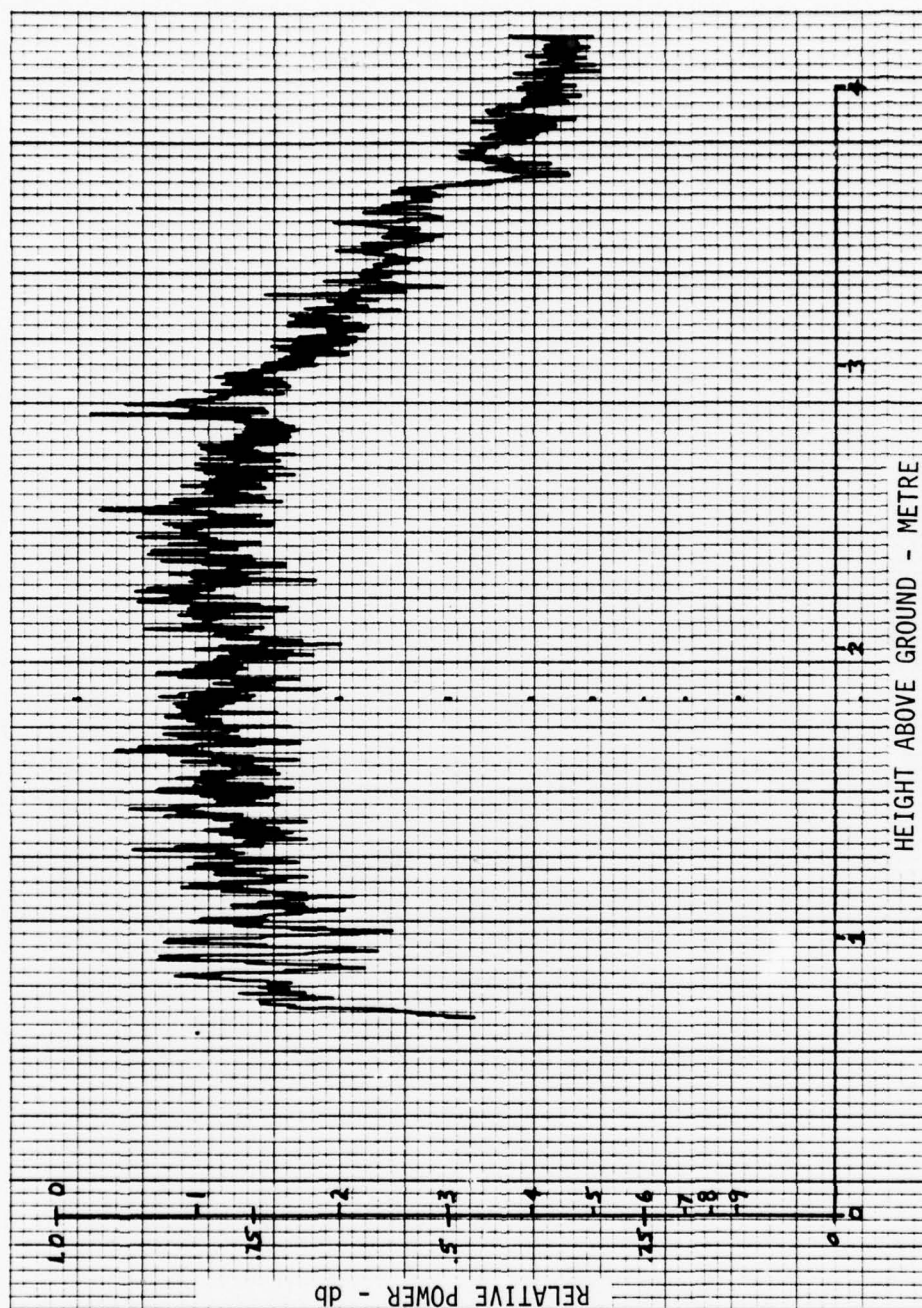


Figure 12. Tracking Pattern - CW, Grass, 50.8-mm Transmitter

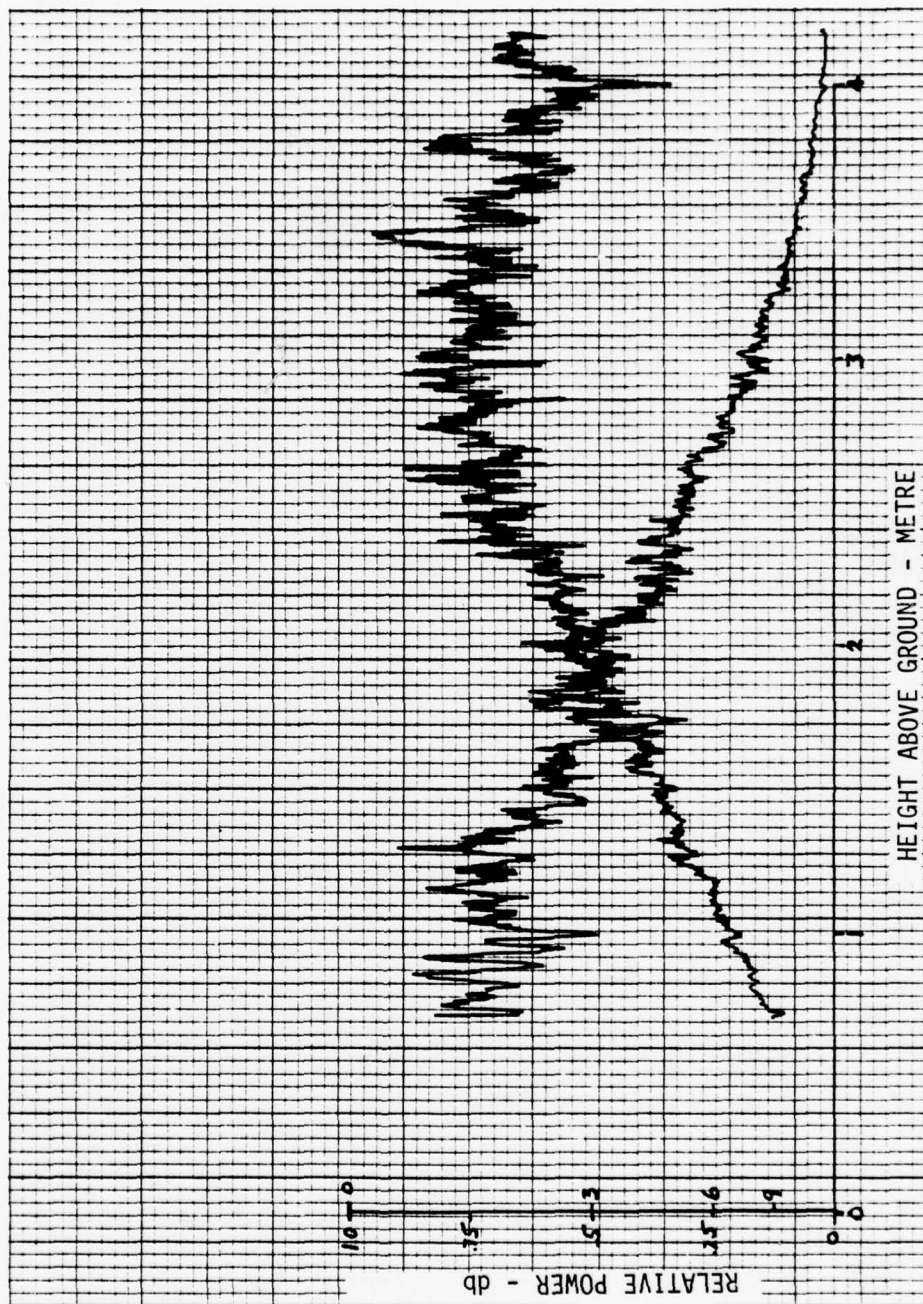


Figure 13. Upper and Lower Lobe Patterns - CW, Grass, 50.8-mm Transmitter

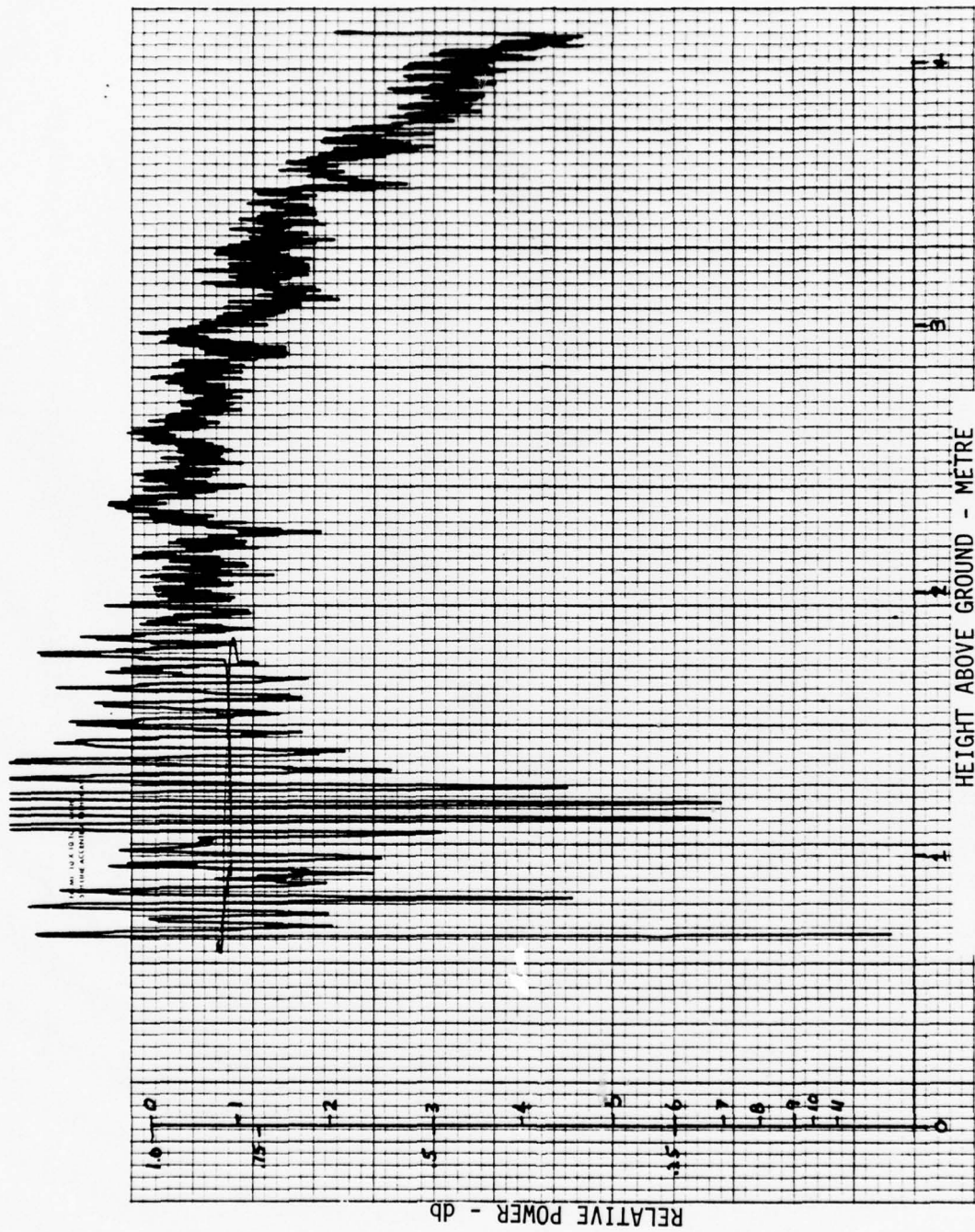


Figure 14. Tracking Pattern - CW, Asphalt, 50.8-mm Transmitter

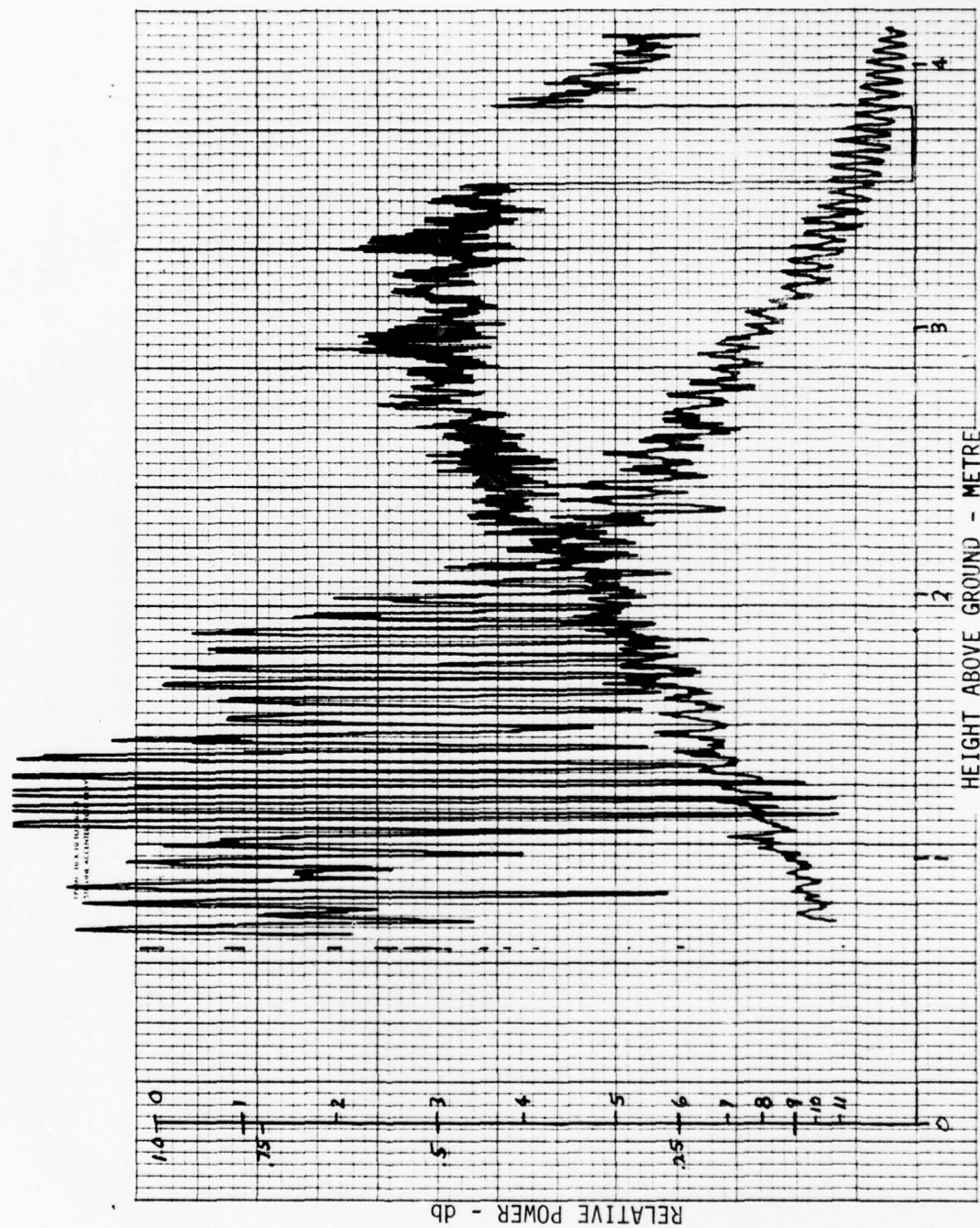


Figure 15. Upper and Lower Lobe Patterns - CW, Asphalt, 50.8-mm Transmitter.
(LO lost from 3.5 to 3.85 m.)

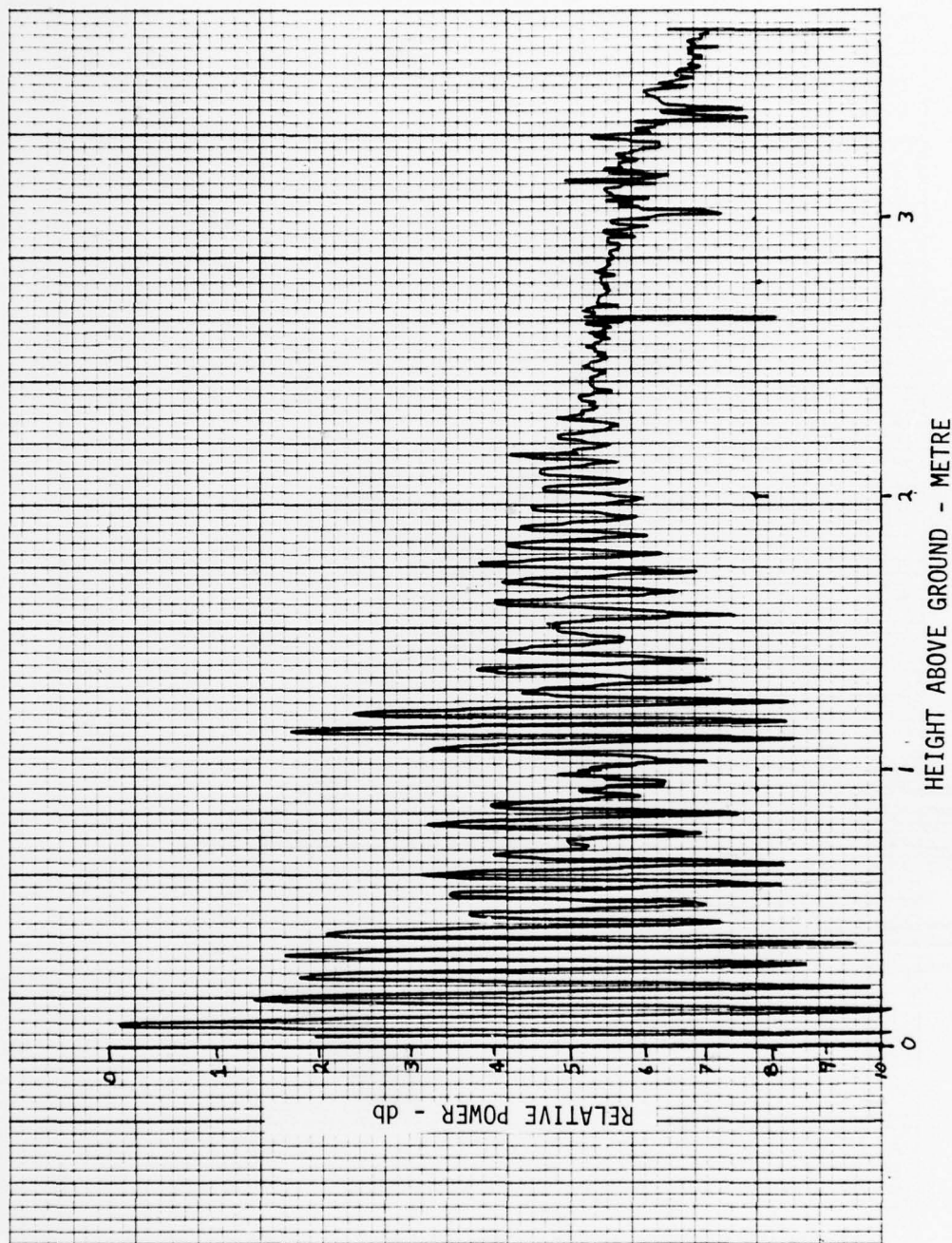


Figure 16. Tracking Pattern - Pulsed, Asphalt, 50.8-mm Transmitter

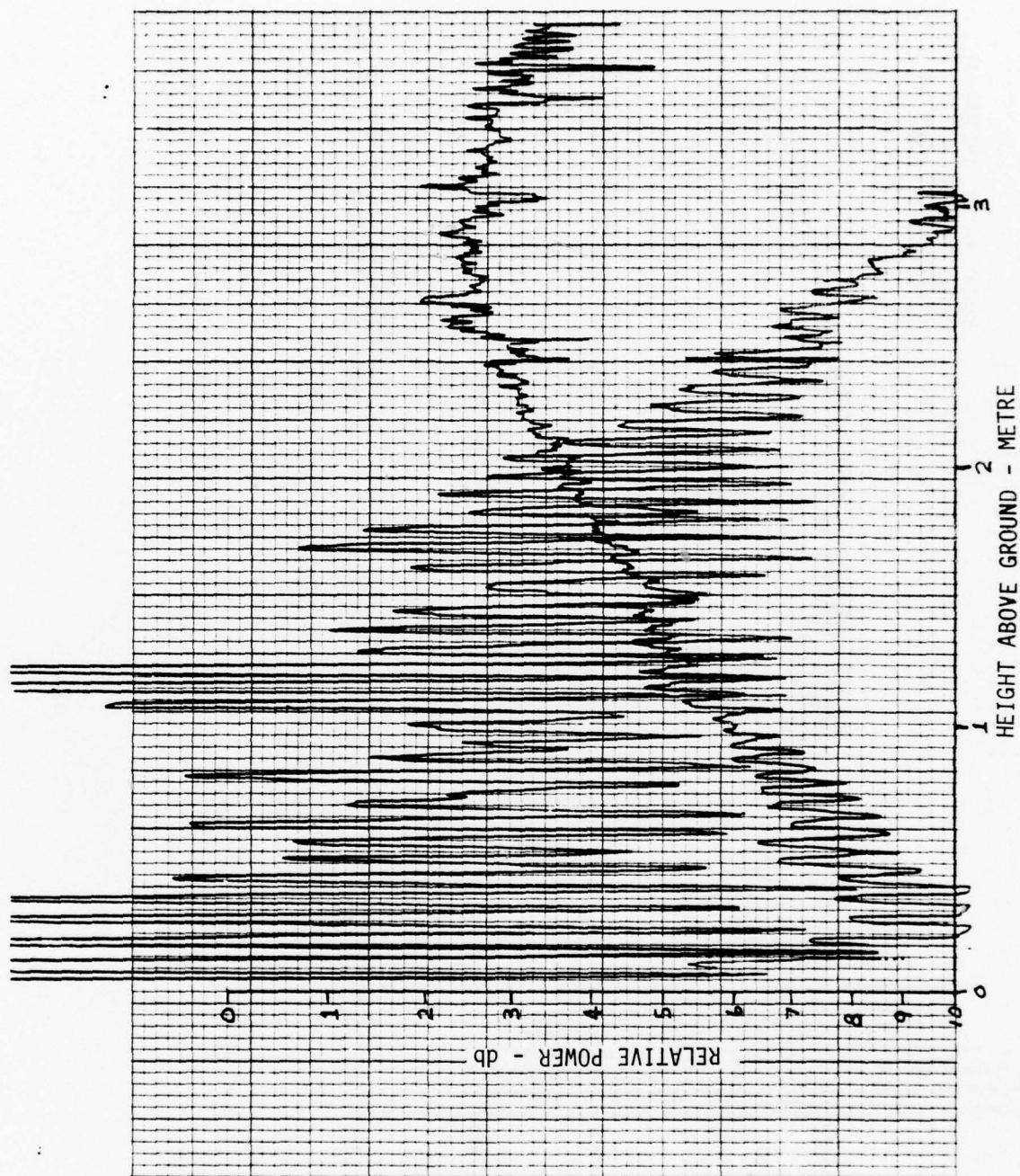


Figure 17. Upper and Lower Lobe Patterns - Pulsed, Asphalt, 50.8-mm Transmitter

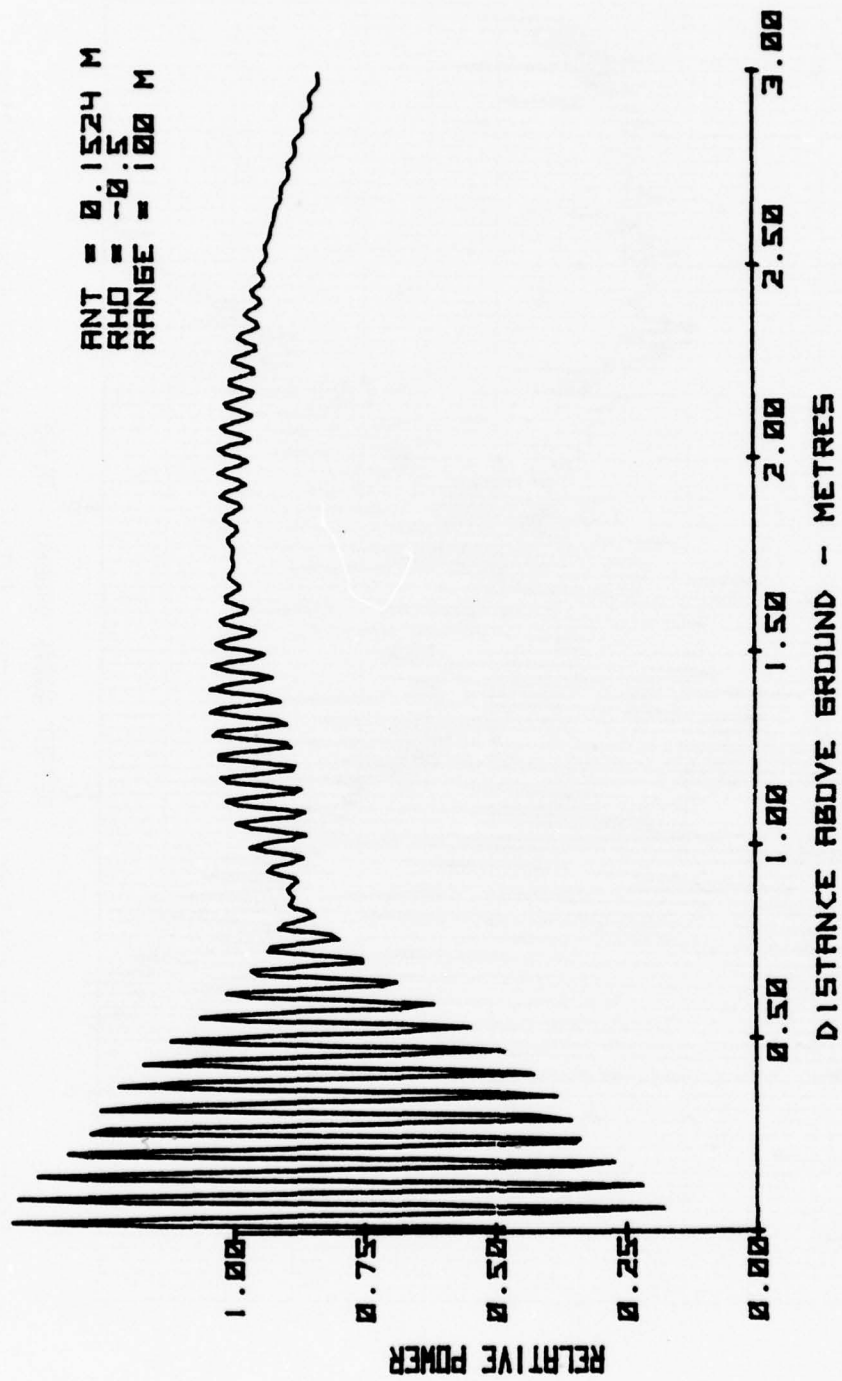


Figure 18. Theoretical Tracking Pattern - 152.4-mm Antenna, $\rho = 0.5$

ANT = 0.1524 M
 RHO = -0.5
 RANGE = 100 M

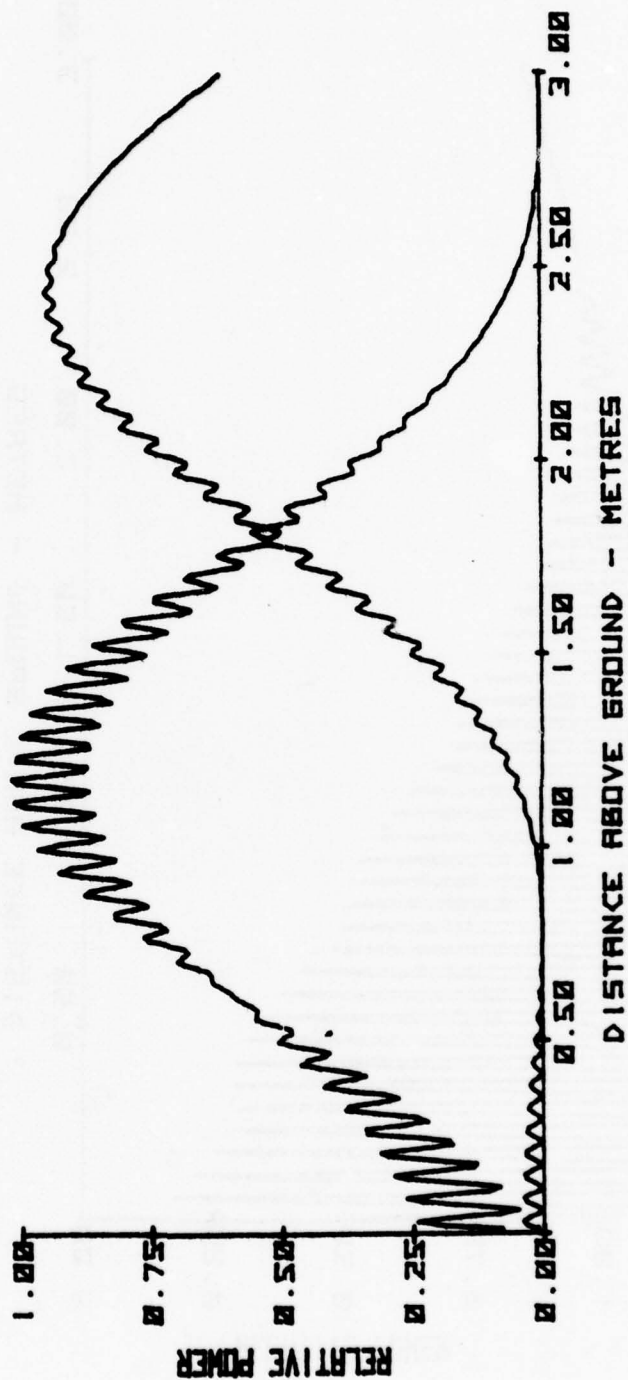


Figure 19. Theoretical Upper and Lower Lobe Patterns - 152.4-mm
 Antenna, $\rho = -0.5$.

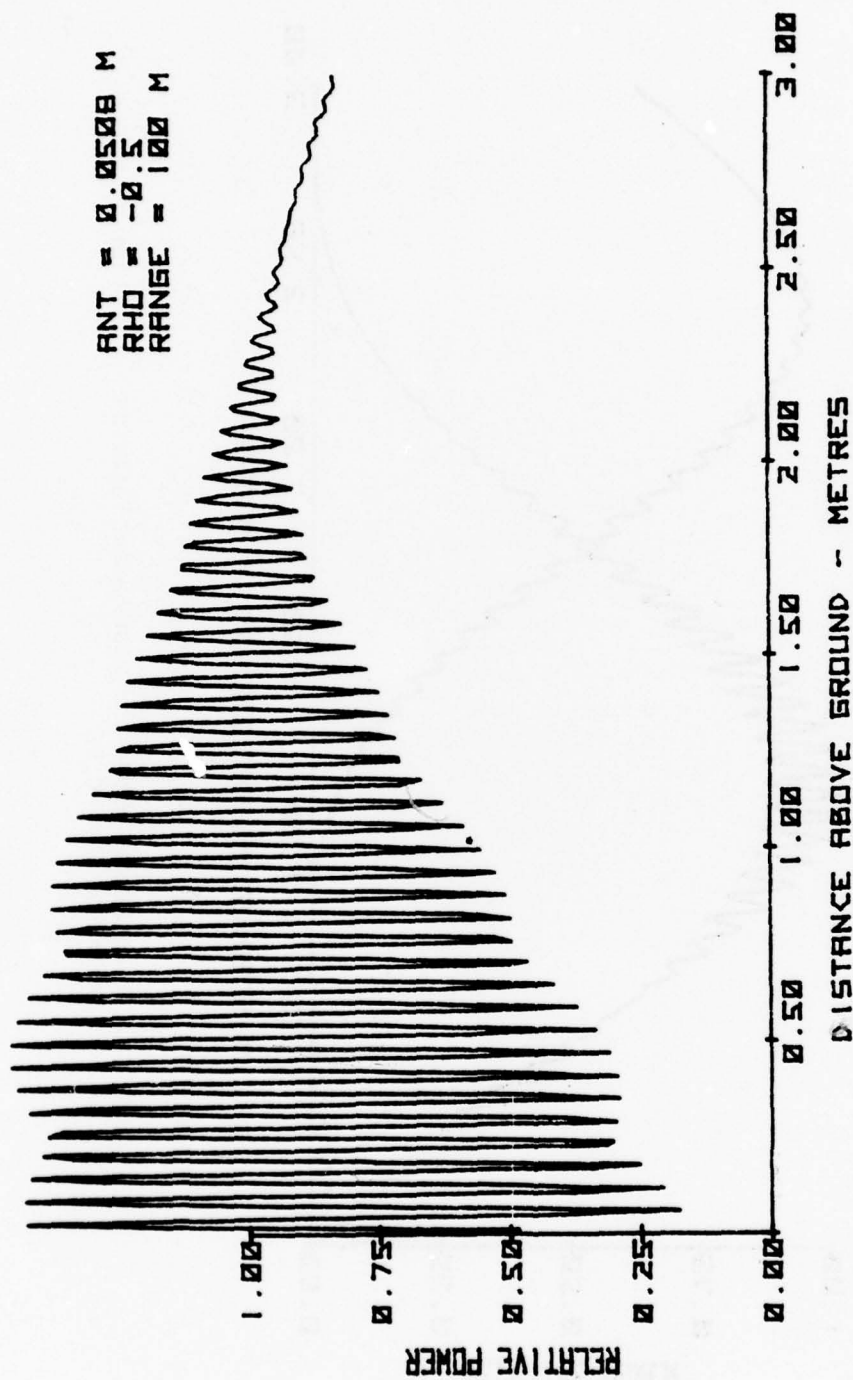


Figure 20. Theoretical Tracking Pattern, 50.8-mm Antenna, $\rho = -0.5$

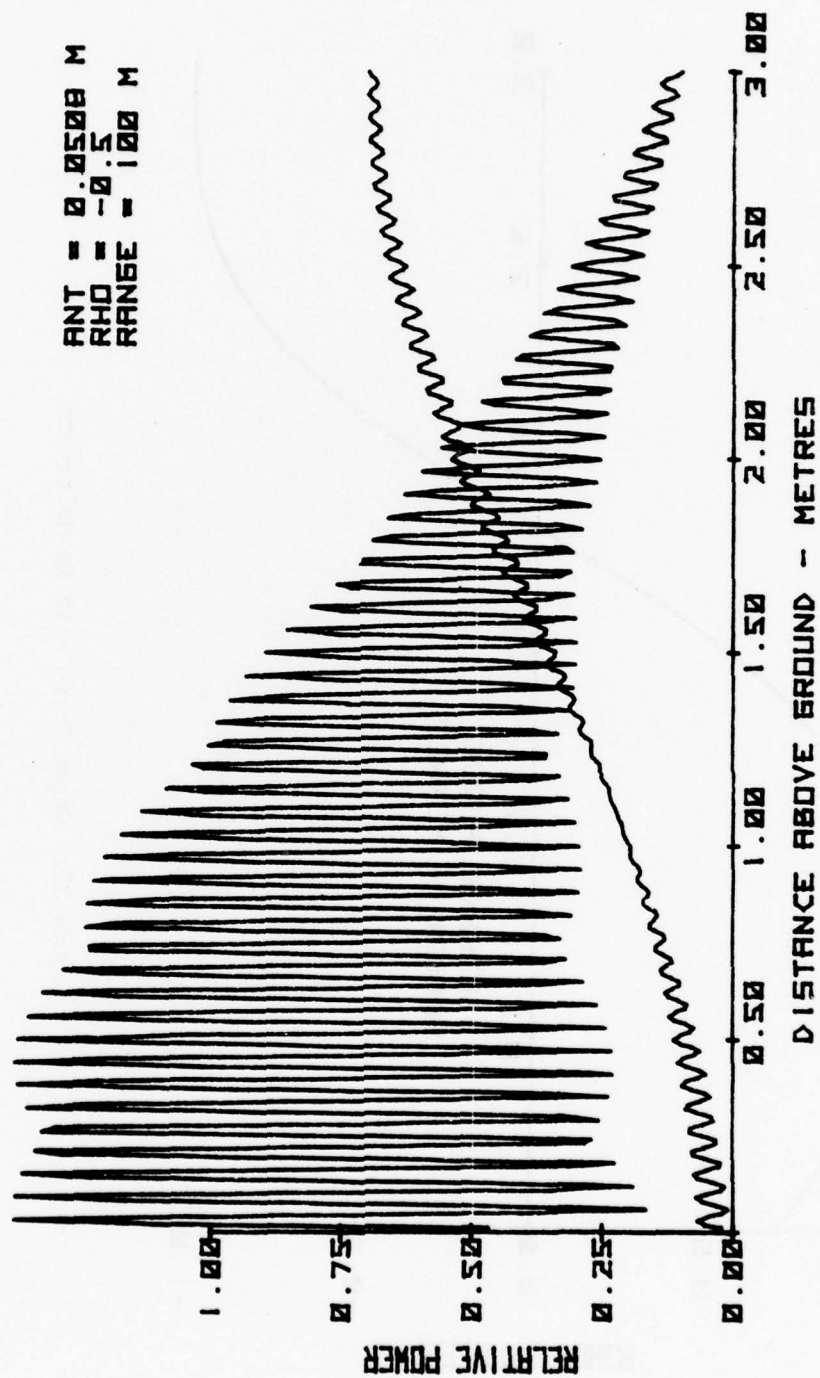


Figure 21. Theoretical Upper and Lower Lobe Patterns, 50.8-mm Antenna,
 $\rho = -0.5$.

ANT = 0.1524 M
 RHO = 0.0
 RANGE = 100 M

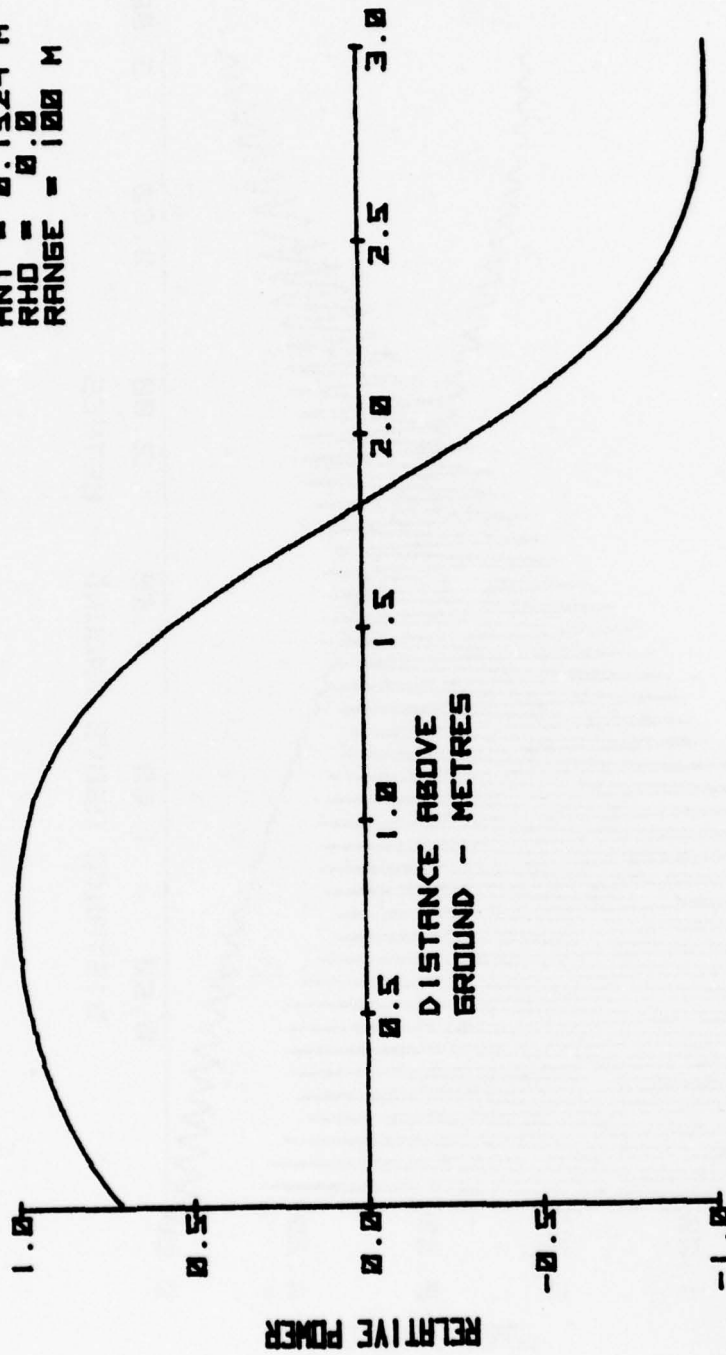


Figure 22. Error Curve with No Multipath

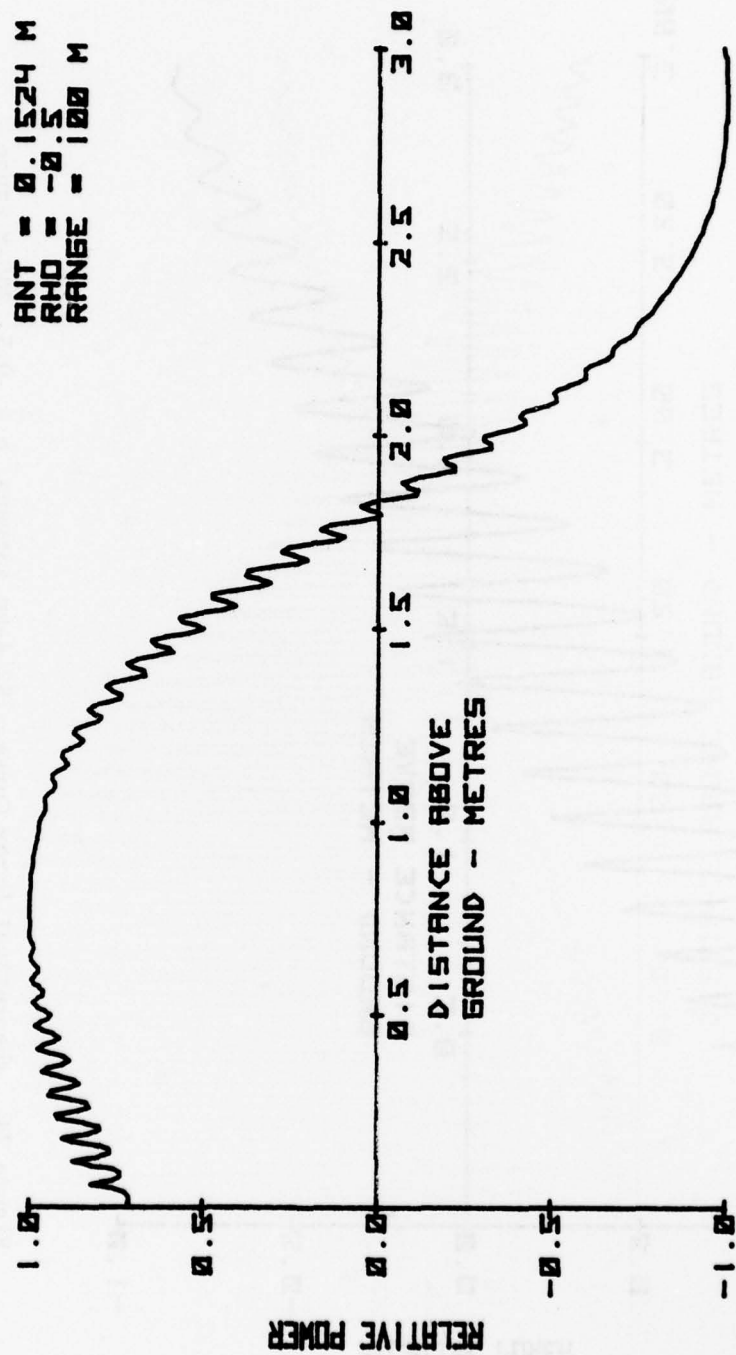


Figure 23. Theoretical Error Curve, 152.4-mm Antenna, $\rho = -0.5$, 100-m Range

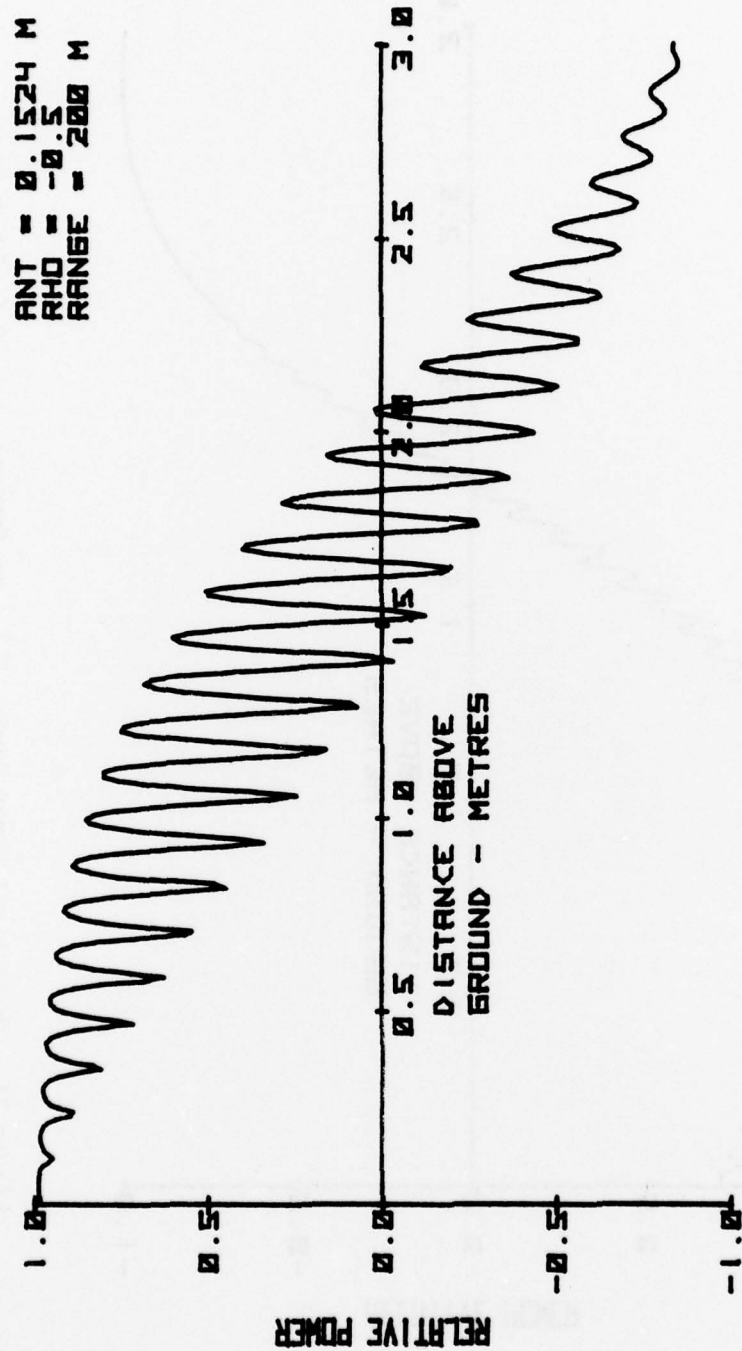


Figure 24. Theoretical Error Curve, 152.4-mm Antenna, $\rho = -0.5$, 200-m Range

ANT = 0.1524 M
 RHO = -0.5
 RANGE = 300 M

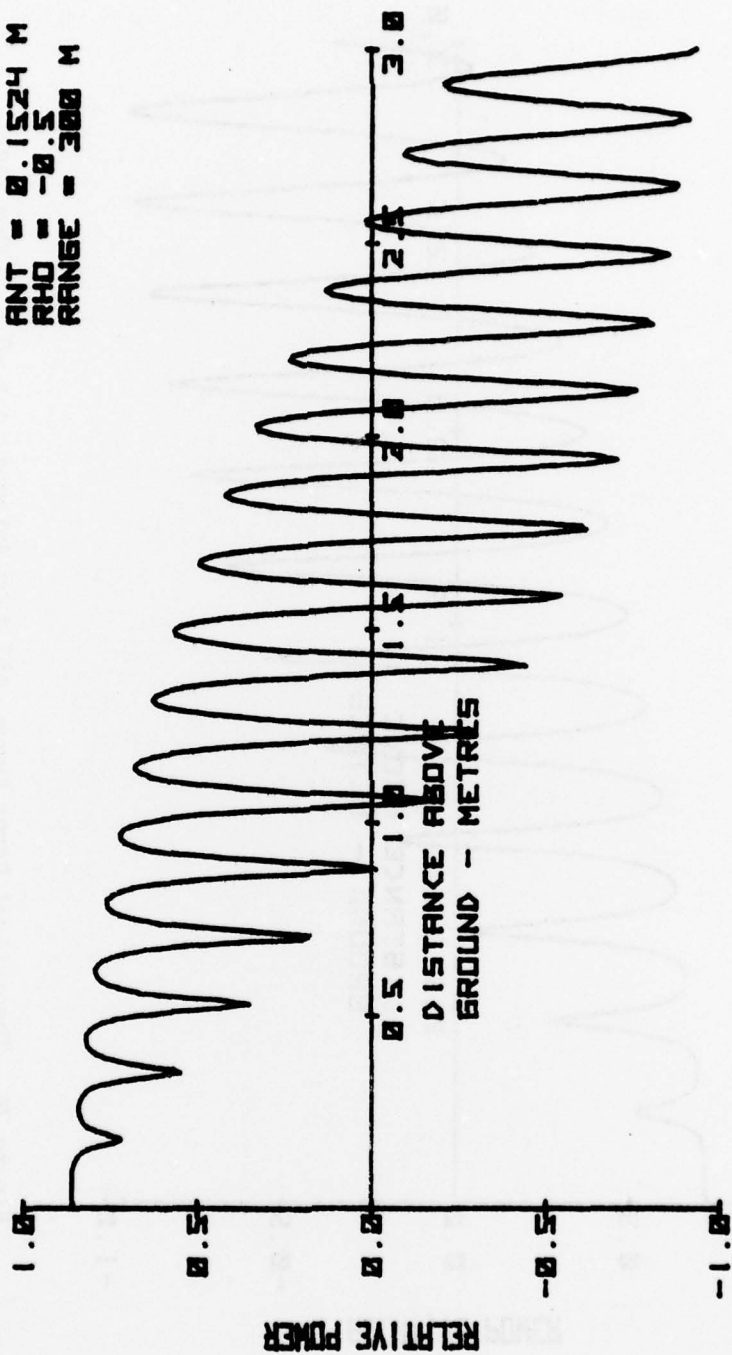


Figure 25. Theoretical Error Curve, 152.4-mm Antenna, $\rho = -0.5$, 300-m Range

ANT = 0.1524 M
 RHD = -0.5
 RANGE = 400 M

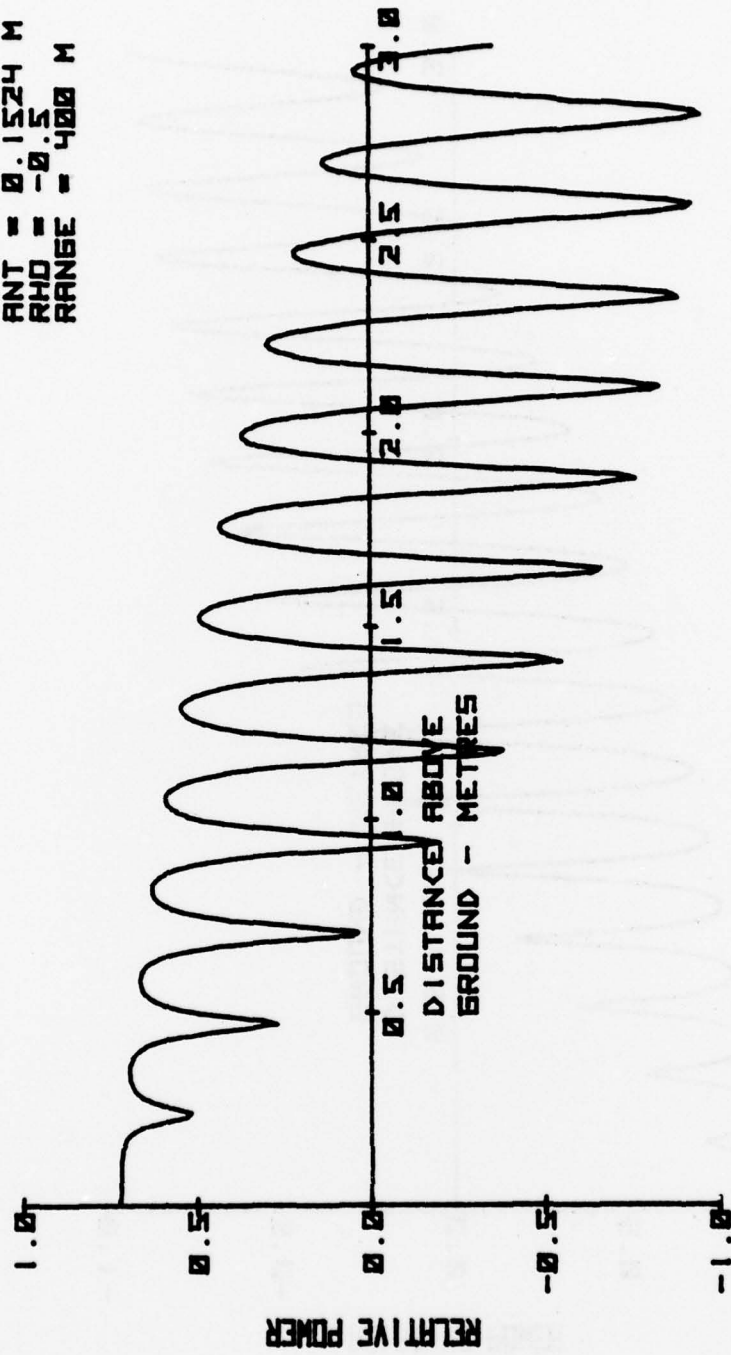


Figure 26. Theoretical Error Curve, 152.4-mm Antenna, $\rho = -0.5$, 400-m Range

ANT = 0.1524 M
 RHD = -0.5
 RANGE = 500 M

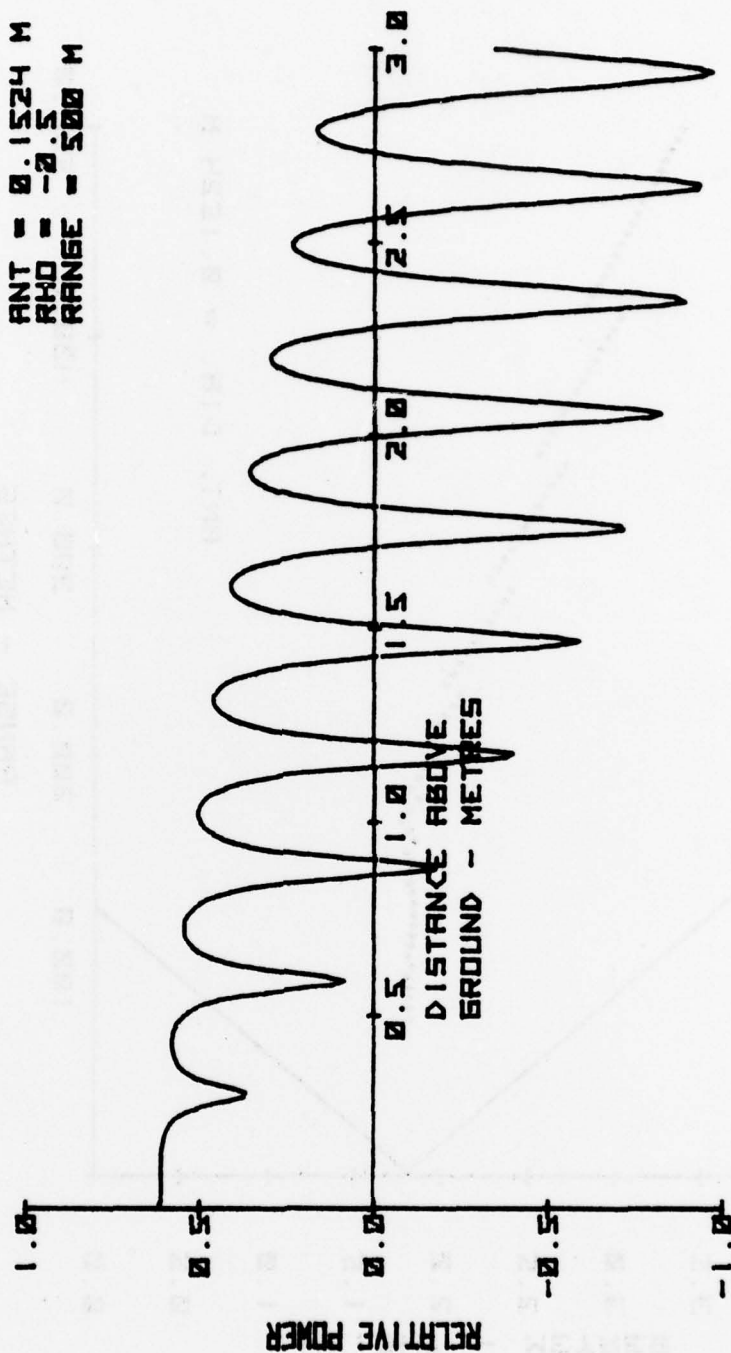


Figure 27. Theoretical Error Curve, 152.4-mm Antenna, $\rho = -0.5$, 500-m Range

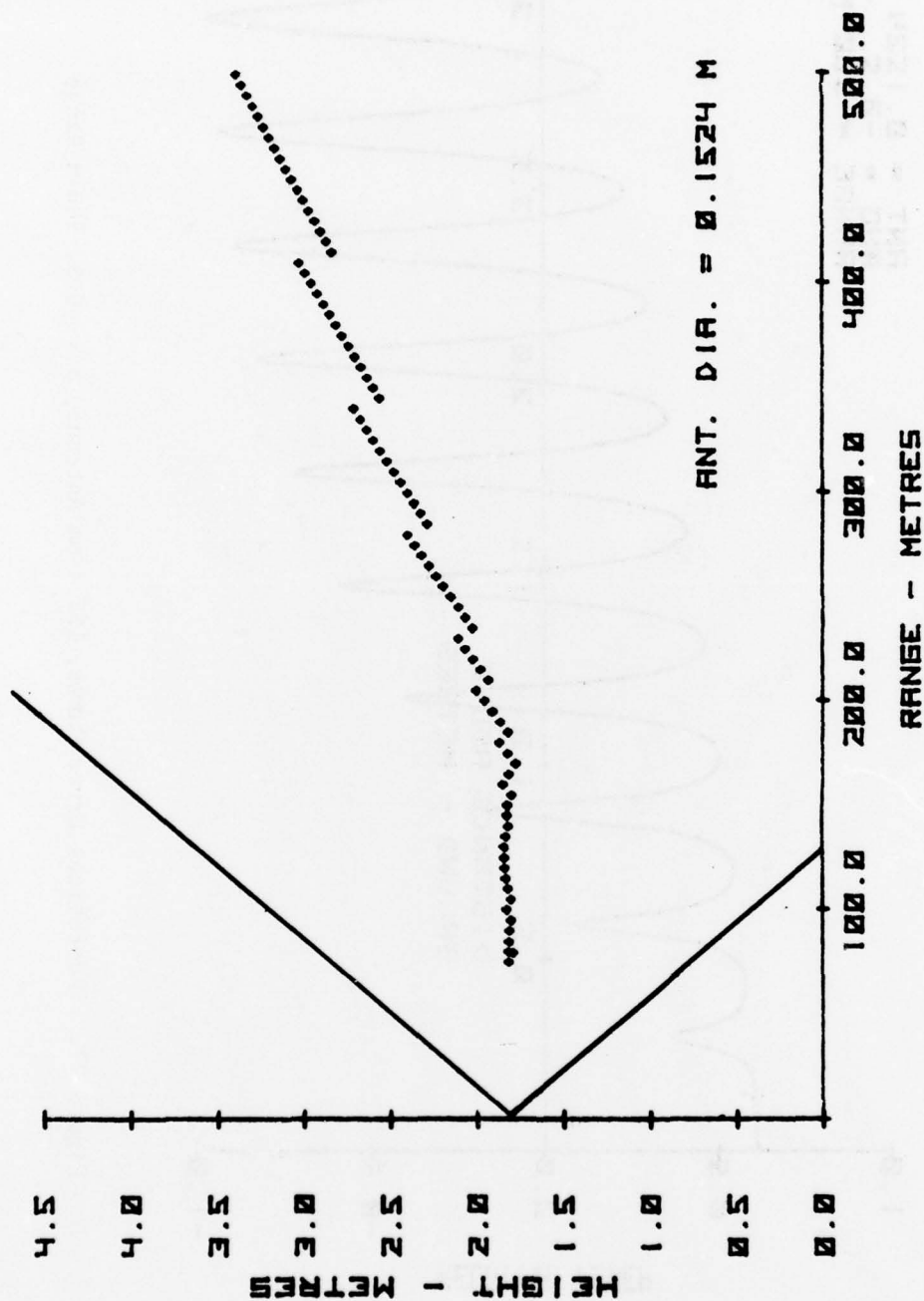


Figure 28. Theoretical Path of "Perfect" Beamrider, Antenna Diameter = 152.4 mm

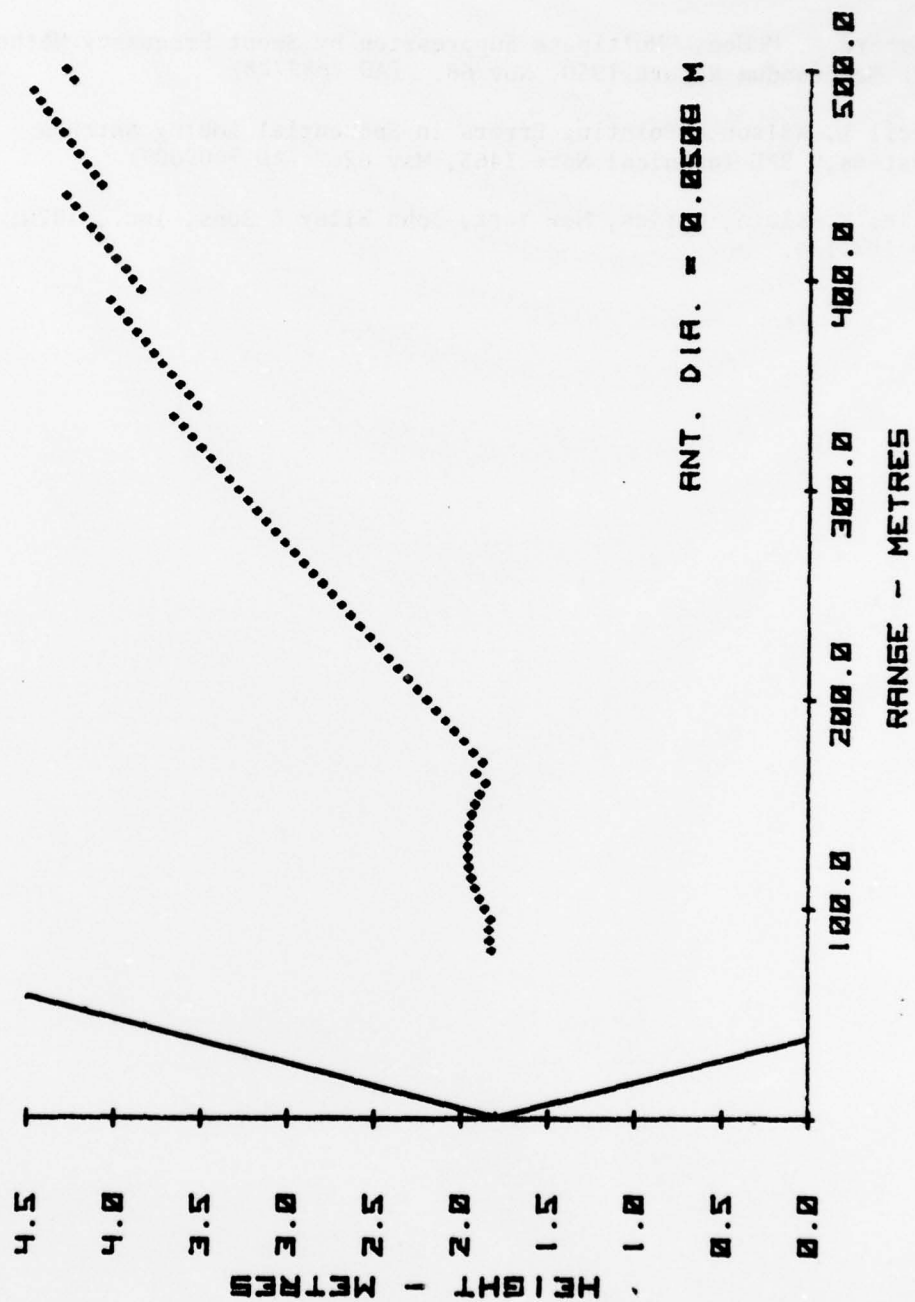


Figure 29. Theoretical Path of "Perfect" Beamrider, Antenna Diameter = 50.8 mm.

REFERENCES

1. David K. Barton, "Low-Angle Radar Tracking," Proc. IEEE, Vol 62, No. 6, Jun 74.
2. Richard A. McGee, "Multipath Suppression by Swept Frequency Methods," BRL Memorandum Report 1950, Nov 68. (AD #682728)
3. Cecil L. Wilson, "Pointing Errors in Sequential Lobing Antenna Systems," BRL Technical Note 1463, May 62. (AD #609009)
4. Miles V. Klein, Optics, New York, John Wiley & Sons, Inc., 1970, pp 184-189.

DISTRIBUTION LIST

<u>No. of Copies</u>	<u>Organization</u>	<u>No. of Copies</u>	<u>Organization</u>
12	Commander Defense Documentation Center ATTN: DDC-TCA Cameron Station Alexandria, VA 22314	1	Commander US Army Aviation Research & Development Command ATTN: DRSAB-E P.O. Box 209 St. Louis, MO 63166
2	Director of Defense Research & Engineering Engineering Technology ATTN: L. Weisberg D. Charvonia Washington, DC 20301	1	Director US Army Air Mobility Research & Development Laboratory Ames Research Center Moffett Field, CA 94035
2	Director Defense Advanced Research Projects Agency ATTN: TTO, J. Tegnalia STO, S. Zakanyycz 1400 Wilson Boulevard Arlington, VA 22209	2	Commander US Army Electronics Research & Development Command ATTN: DRDEL-AP-CCM, D. Giglio DRDEL-AP-FI, D. Gormley 2800 Powder Mill Road Adelphi, MD 20783
1	Director Institute for Defense Analyses ATTN: V. Corcoran 400 Army-Navy Drive Arlington, VA 22202	4	Commander US Army Electronics Research & Development Command Technical Support Activity ATTN: DELSD-L DRDEL-CT DRDEL-RD DRDEL-VT, Mr. Post Fort Monmouth, NJ 07703
1	Director Defense Nuclear Agency ATTN: STRA (RAEL) Washington, DC 20305	5	Commander US Army Electronics Research & Development Command Technical Support Activity ATTN: DELET-MJ, H. Jacobs A. Kerecman DELCS-R-CSTA, R. Pearce DELNV-L, R. Buser R. Rohde Fort Monmouth, NJ 07703
2	Commander US Army Materiel Development & Readiness Command ATTN: DRCDMD-ST, N. Klein DRCBSI, P. Dickinson 5001 Eisenhower Avenue Alexandria, VA 22333		

DISTRIBUTION LIST

<u>No. of Copies</u>	<u>Organization</u>	<u>No. of Copies</u>	<u>Organization</u>
1	Commander US Army Electronics Research & Development Command ATTN: DRDEL-BL-RD, Atmos Sci Rsch Fort Huachuca, AZ 85613	7	Commander US Army Missile Research & Development Command ATTN: DRDMI-TR, R. Hartman DRDMI-TRO, B. Guenther W. Gamble DRDMI-REO, G. Emmons DRDMI-R, Mr. Pittman DRDAR-RBL DRDAR-RES Redstone Arsenal, AL 35809
8	Commander US Army Harry Diamond Laboratories ATTN: DELHD-NMM, E. Brown S. Kulpa B. Weber DELHD-RA, J. Salerno DELHD-RAC, R. Humphrey DELHD-RCB, G. Simonis DELHD-DBE, T. Gleason DELHD-TD 2800 Powder Mill Road Adelphi, MD 20783	6	Commander US Army Missile Research & Development Command ATTN: DRDMI-RER, H. Green DRDMI-R DRDMI-RF, C. Hussey DRDMI-RFC, A. Michetti DRDMI-RFE, Mr. Duvall Mr. Salonimer Redstone Arsenal, AL 35809
1	Director US Army Atmospheric Sciences Laboratory ATTN: DRSEL-BL-AS-P, K. White White Sands Missile Range, NM 88002	1	Commander US Army Missile Materiel Readiness Command ATTN: DRSMI-AOM Redstone Arsenal, AL 35809
1	Office of Test Director Joint Services LGW/CM Test Program ATTN: DRDEL-WL-MT, R. Murray White Sands Missile Range, NM 88002	1	Commander US Army Mobility Equipment Research & Development Command ATTN: SMEFB-EM, K. Steinback Fort Belvoir, VA 22060
2	Director US Army Night Vision Laboratory ATTN: DRSEL-NV-VI, J. Moulton DRSEL-NV-II, R Shurtz Fort Belvoir, VA 22060	1	Commander US Army Tank Automotive Research & Development Command ATTN: DRDTA-UL Warren, MI 48090
1	Commander US Army Communication Research & Development Command ATTN: DRDCO-SGS Fort Monmouth, NJ 07703		

DISTRIBUTION LIST

<u>No. of</u> <u>Copies</u>	<u>Organization</u>	<u>No. of</u> <u>Copies</u>	<u>Organization</u>
5	Commander US Army Armament Research & Development Command ATTN: DRDAR-TSS (2 cys) DRDAR-SC, J. Schmitz R. Pfeilsticker DRDAR-LCU-DE, T. Malgeri Dover, NJ 07801	1	HQDA (DAMA-CSM-CA/LTC N. Conner) WASH DC 20310
		1	HQDA (DAMA-DDZ-C) WASH DC 20310
1	Commander US Army Armament Materiel Readiness Command ATTN: DRSAR-LEP-L, Tech Lib Rock Island, IL 61202	1	Commander US Army Ballistic Missile Defense Advanced Technology Center ATTN: BMD-ATC-D, C. Johnson P.O. Box 1500 Huntsville, AL 35807
1	Commander US Army White Sands Missile Range ATTN: STEWS-TE, J. Flores White Sands Missile Range, NM 88002	2	Commander US Army Research Office ATTN: D. Van Hulsteyn R. Lontz P.O. Box 12211 Research Triangle Park, NC 27709
1	Commander US Army Foreign Science & Technology Center ATTN: DRXST-SD, O. Harris 220 7th Street, NE Charlottesville, VA 22901	1	Director US Army Research & Development Group (Europe) ATTN: Elct Br Box 15 FPO New York, NY 09510
1	Commander US Army TRADOC Systems Analysis Activity ATTN: ATAA-SL, Tech Lib White Sands Missile Range NM 88002	1	Commander US Naval Air Systems Command ATTN: AIR-2324, C. Francis Washington, DC 20360
1	Commander TCATA ATTN: Scientific Advisor Fort Hood, TX 76544	1	Chief of Naval Research Department of the Navy Washington, DC 20360
		2	Commander US Naval Air Development Center ATTN: AETD, Radar Div Mr. M. Foral Warminster, PA 18974
1	HQDA (SARD) Assistant for Electronics ATTN: V. Friedrich WASH DC 20310		

DISTRIBUTION LIST

<u>No. of</u> <u>Copies</u>	<u>Organization</u>	<u>No. of</u> <u>Copies</u>	<u>Organization</u>
1	Commander Center for Naval Analyses ATTN: Docu Control 1401 Wilson Boulevard Arlington, VA 22209	1	ADTC/DLMT Eglin AFB, FL 32542
2	Commander Naval Electronics Lab Center ATTN: Code 2330, J.Provencher Tech Lib San Diego, CA 92152	1	ADTC/ADA Eglin AFB, FL 32542
2	Commander Naval Surface Weapons Center ATTN: Lib Code DF34 Dahlgren, VA 22448	1	AFATL/DLB Eglin AFB, FL 32542
3	Commander Naval Weapons Center ATTN: Code 6014, J. Battles R. Moore R. Higuera China Lake, CA 93555	1	AFATL/DLTG, F. Prestwood Eglin AFB, FL 32542
3	Commander Naval Research Laboratory ATTN: Code 5300, Radar Div. Dr. Skolnik Code 5370, Radar Geophysics Br. Code 5460, EM Prop Br. Washington, DC 20375	2	AFATL (DLYW/DLDG) Eglin AFB, FL 32542
3	Commander Naval Research Laboratory ATTN: Code 7110, B. Yaplee Code 7122.1, K. Shivanandan Code 7111, J. Hollinger Washington, DC 20375	1	RADC/EMATE Griffiss AFB, NY 13440
1	ADTC/ADBPS-12 Eglin AFB, FL 32542	1	RADC/ETEN, E. Altshulder Griffiss AFB, NY 13440
		3	AFGL/LZ, C. Sletten; LZN, E. Altschuler; S. Clough Hanscom AFB, MA 01730
		1	AFAL/WRW, Mr. Leasure Kirtland AFB, NM 87117
		1	AFWL/DEV Kirtland AFB, NM 87117
		1	AFAL/RWN-1, R. Bruns Wright-Patterson AFB, OH 45433
		1	Director National Bureau of Standards ATTN: Div 276.106, C. Miller Boulder, CO 80302

DISTRIBUTION LIST

<u>No. of</u> <u>Copies</u>	<u>Organization</u>	<u>No. of</u> <u>Copies</u>	<u>Organization</u>
1	Director National Oceanographic & Atmospheric Administration ATTN: V. Derr Boulder, CO 80303	2	Hughes Aircraft Company Aerospace Group Electron Dynamic Division ATTN: N. Kramer J. Sparacio 3100 West Lomita Boulevard Torrance, CA 90504
2	The Ivan A. Getting Laboratory The Aerospace Corporation ATTN: T. Hartwick D. Hodges P.O. Box 92957 Los Angeles, CA 90009	1	Martin Marietta Corporation ATTN: M. Wiltse P.O. Box 5837 Orlando, FL 32805
1	Ford-Aeronutronic ATTN: D. Burch Ford Road Newport, CA 92663	1	The Rand Corporation ATTN: S. Dudzinsky 1700 Main Street Santa Monica, CA 90406
1	Goodyear Aerospace Corporation Arizona Division ATTN: F. Wilcox Litchfield Park, AZ 85340	1	R&D Associates ATTN: G. Gordon P.O. Box 9695 Marina Del Rey, CA 90291
1	Honeywell Corporate Research Ctr ATTN: P. Kruse 10701 Lyndale Avenue South Bloomington, MN 55420	1	Raytheon Company Missiles Systems Division ATTN: W. Justice Hartwell Road Bedford, MA 01730
1	Honeywell, Inc. Systems and Research Division ATTN: C. Seashore 2700 Ridgway Parkway Minneapolis, MN 55413	1	Sperry Rand Corporation Microwave Electronics Division ATTN: R. Roder Clearwater, FL 33518
1	Hughes Aircraft Company Aerospace Group Advanced Program Development Systems Division ATTN: M. Bebe Canoga Park, CA 91304	1	United Aircraft Corporation Norden Division ATTN: Dr. L. Kosowsky Helen Street Norwalk, CT 06852
1	Hughes Aircraft Company Aerospace Group Radar Division ATTN: R. Wagner Culver City, CA 90230	2	University of Illinois Department of Electrical Engineering EERL-200 ATTN: T. DeTemple P. Coleman Urbana, IL 61801

DISTRIBUTION LIST

<u>No. of Copies</u>	<u>Organization</u>
2	Director Applied Physics Laboratory The Johns Hopkins University ATTN: A. Stone Lib Johns Hopkins Road Laurel, MD 20810
4	Georgia Institute of Technology Engineering Experiment Station ATTN: R. Hayes F. Dyer J. Dees J. Gallagher 347 Ferst Drive Atlanta, GA 30332
1	Lincoln Laboratory, MIT ATTN: C. Blake P.O. Box 73 Lexington, MA 02173
1	Francis Bitter National Magnet Lab, MIT ATTN: K. Button 170 Albany Street Cambridge, MA 02139

Aberdeen Proving Ground

Dir, USAMSAA
Cdr, USATECOM
ATTN: DRSTE-SG-H
J. Phillips
Cdr, APG
ATTN: STEAP-MT-TF
W. Frazier
S. Taragin

